Advances in Dielectric Elastomers for Actuators and Artificial Muscles

Paul Brochu, Qibing Pei*

A number of materials have been explored for their use as artificial muscles. Among these, dielectric elastomers (DEs) appear to provide the best combination of properties for true muscle-like actuation. DEs behave as compliant capacitors, expanding in area and shrinking in thickness when a voltage is applied. Materials combining very high energy densities, strains, and efficiencies have been known for some time. To date, however, the widespread adoption of DEs has been hindered by premature breakdown and the requirement for high voltages and bulky support frames. Recent advances seem poised to remove these restrictions and allow for the production of highly reliable, high-performance transducers for artificial muscle applications.

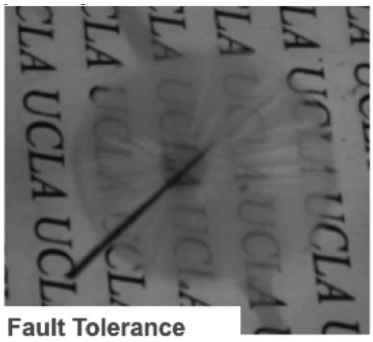

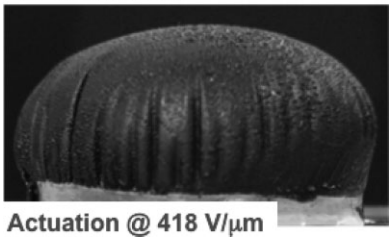

Introduction

The ability to mimic the muscles in our own human bodies, both for the advancement in our well being and for our amusement, has been a topic of great interest for some time. Natural muscle has a number of properties that make it difficult to match in terms of performance. The energy density of muscle is on the order of 150 $J \cdot kg^{-1}$ and can peak at around 300 $J \cdot kg^{-1}$,[1] while displacements are relatively large with typical strains ranging from 20 to 40% and peaking at 100%.[2–4] By these measures alone, electromagnetic (EM) motors and combustion engines should be able to match or exceed the performance of natural muscle.[5] However, as it is made obvious by current leading-edge robots (e.g., Honda's Asimo),[6] the real world performance of conventional-actuator-based robotics is limited.[2,7] The shortcoming lies on several fronts, first is the power supply: natural muscle relies on chemical energy that is supplied to living organisms through the ingestion of food, while EM motors rely on heavy battery pack and capacitor banks that must be recharged frequently. These large power sources contribute to the overall mass of the robotic device and reduce the effective energy density as well as limit range and mobility. Second is the requirement for gearing systems: EM motors operate best at high rotational speeds; these must be reduced significantly through the use of gearing systems that can significantly increase mass and reduce energy density. Third is the ability to recover energy: tendon and flesh, as well as muscle itself, are capable of absorbing and storing a large percentage of the impact energy that can be translated back to motion. Additionally, muscles possess other salient properties that allow them to operate as motors, brakes, springs, and struts, permitting better stability control and impact energy absorption.[8] EM motors also generate more noise and heat than natural muscle, which is not welcome

Q. Pei, P. Brochu
Department of Materials Science and Engineering, The Henry Samueli School of Engineering, University of California, 420 Westwood Plaza, Los Angeles, CA 90095-1595, USA
Fax: (+1) 310 206 7353; E-mail: qpei@seas.ucla.edu

Macromol. Rapid Commun. **2010**, *31*, 10–36

DOI: 10.1002/marc.200900425

Paul Brochu is a Ph.D. candidate at the University of California Los Angeles. He is currently working on dielectric elastomers for energy harvesting in the Soft Materials Research Laboratory. Paul received his Bachelors of Applied Science in nanoengineering at the University of Toronto in Toronto, Ontario, Canada. He received his Masters in materials science and engineering from the University of California Los Angeles in electronic materials.

Qibing Pei is professor of materials science and engineering specializing in synthetic polymers. He worked successively as a senior chemist at UNIAX Corporation, Santa Barbara, CA, which was later merged into DuPont Display, a senior chemist at Imation Corporation, Santa Paul, MN, and a senior research engineer at SRI International, Menlo Park, CA. He has developed a number of electronic and electroactive polymers for applications in electro-optic and electro-mechanical devices, including light emitting diodes, polymer light emitting electrochemical cells, electroactive polymer artificial muscles, and biologically inspired robots. His research interests cover a wide range of soft materials and span from material synthesis, processing, to design of functional devices. He applies organic synthesis, polymer synthesis, solution-based processing, and nanofabrication in the discovery of new polymers and multifunctional composites.

for certain applications, and cannot be effectively operated in large magnetic fields.

Pneumatic systems operate linearly like natural muscle; pneumatic artificial muscles (McKibben artificial muscles) in particular are intrinsically compliant and can thus provide the "give" that natural muscle is capable of. Unfortunately, these systems require air compressors that are neither light nor small, and their response speed is limited by the ability to pump air into and out of the actuators.

Several "smart materials" have been proposed as artificial muscles, these include shape memory alloys (SMAs), magnetostrictive alloys (MSAs), and piezoelectrics.[2,9] SMAs are capable of producing relatively large linear displacements and can be actuated relatively quickly using resistive heating. What limits their applicability to artificial muscle applications is the time it takes to cool the alloy and return to the rest position. In order to obtain good operating frequencies, the SMA must be actively cooled, increasing the bulk, complexity, and cost of the system. MSAs and piezoelectric ceramics both suffer from small strains and high stiffness. These materials are thus not particularly suited to artificial muscle applications.

Polymers present an interesting alternative to conventional technologies. They possess inherent compliance, are lightweight, and are generally low cost. Electroactive polymers (EAPs) are an emerging type of actuator technology wherein a lightweight polymer responds to an electric field by generating mechanical motion.[1,10,11] Their ability to mimic the properties of natural muscle has garnered them the moniker artificial muscle, though the term electroactive polymer artificial muscle (EPAM) is more appropriate and descriptive.

The concept of EAPs can be dated back to 1880 in a paper by Roentgen.[12] In his experiments, he observed that a film of natural rubber could be made to change in shape by applying a large electric field across it; this was the first observation of actuation of a dielectric elastomer (DE) material.

Today the number of EAPs has grown substantially. There currently exists a wide variety of such materials, ranging from rigid carbon nanotubes (CNTs) to soft DEs. A number of reviews and overviews have been prepared on these and other materials for use as artificial muscles and other applications.[1,2,7,10,11,13–28] The next section will provide a survey of the most common electrically activated EAP technologies and provide some pertinent performance values. The remainder of the paper will focus specifically on DEs. Several actuation properties for these materials are summarized in Table 1 along with other actuation technologies including mammalian muscle. It is important to note that data were recorded for different materials under different conditions so the information provided in the table should only be used as a qualitative comparison tool.

Survey of EAP Technologies

EAPs can be broadly divided into two categories based on their method of actuation: ionic and field-activated. Further subdivision based on their actuation mechanism and the type of material involved is also possible. Ionic polymer–metal composites, ionic gels, CNTs, and conductive polymers (CPs) fall under the ionic classification. Ferroelectric polymers, polymer electrets, electrostrictive polymers, and DEs fall under the electronic classification.

Ionic EAPs

Ionic Polymer–Metal Composites

Ionic polymer–metal composites (IPMCs) consist of a solvent swollen ion-exchange polymer membrane laminated between two thin flexible metal (typically percolated Pt nanoparticles or Au) or carbon-based electrodes.[1,29,30] Application of a bias voltage to the device causes the

Table 1. Comparison of actuator materials.

Type (specific)	Maximum strain	Maximum pressure	Specific elastic energy density	Elastic energy density	Coupling efficiency k^2	Maximum efficiency	Specific density	Relative speed (full cycle)	References
	%	MPa	$J \cdot g^{-1}$	$J \cdot cm^{-3}$	%	%			
Dielectric elastomer (acrylic with prestrain)	380	7.2	3.4	3.4	85	60–80	1	Medium	[2,3,164]
Dielectric elastomer (silicone with prestrain)	63	3	0.75	0.75	63	90	1	Fast	[164]
Dielectric elastomer (silicone — nominal prestrain)	32	1.36	0.22	0.2	54	90	1	Fast	[3]
Electrostrictive polymer [P(VDF–TrFE)]	4.3	43	0.49	0.92	–	≈80 (est.)	1.8	Fast	[3]
Electrostatic devices (integrated force array)	50	0.03	0.0015	0.0025	50 (est.)	>90	1	Fast	[3,4,164]
Electromagnetic (voice coil)	50	0.1	0.003	0.025	–	>90	8	Fast	[3,4]
Piezoelectric ceramic (PZT)	0.2	110	0.013	0.1	52	>90	7.7	Fast	[3]
Piezoelectric single crystal (PZT-PT)	1.7	131	0.13	1	81	>90	7.7	Fast	[3]
Piezoelectric polymer (PVDF)	0.1	4.8	0.0013	0.0024	7	–	1.8	Fast	[3]
Shape memory alloy (TiNi)	>5	>200	>15	>100	5	<10	6.5	Slow	[3]
Shape memory polymer (polyurethane)	100	4	2	2	–	<10	1	Slow	[3]
Thermal (expansion — Al, dT = 500 K)	1	78	0.15	0.4	–	<10	2.7	Slow	[3]
Conducting polymer (PANI)	10	450	23	23	<1	<5 (est.)	≈1	Slow	[3,4]
Ionic gels (polyelectrolyte)	>40	0.3	0.06	0.06	–	30	≈1	Slow	[3]
Magnetostrictive (terfenol-D)	0.2	70	0.0027	0.025	–	60	9	Fast	[3]
Natural muscle (human skeletal)	>40	0.35	0.07	0.07	–	>35	1	Medium	[3]
Natural muscle (peaks in nature)	100	0.8	0.04	0.04	–	40	–	Slow–fast	[2,4]

migration of mobile ions within the film to the oppositely charged electrode causing one side of the membrane to swell and the other to contract resulting in a bending motion.[31] Over time the actuator will relax slightly due to the built-up pressure gradient. A schematic representation of the actuation mechanism is shown in Figure 1. Typical membrane materials include Nafion and Flemion[20] with anionic side groups or polystyrene (PS) ionomers with anionic-substituted phenyl rings.[1,2,29] Wang et al.[32] have recently shown that IPMCs based on a sulfonated poly(styrene-*block*-ethylene-*co*-butylene-*block*-styrene) ionic membrane are capable of high speed bending actuation under constant voltages and give excellent harmonic responses under sinusoidal excitation. Since the membrane materials contain anionic species they will be negatively charged, so cationic species are added to the solvent in the membrane to balance the charge. The ionic segments of the chains form hydrophilic clusters whereas the surrounding areas are hydrophobic; as such the mobile ions accumulate near the ionic segments. Channels through the hydrophobic regions allow for ion and solvent migration.[33] Driving voltages are typically on the order of a few volts or less and actuation strains and stresses of >3%[30,34] and 30 MPa[29,33] have been reported. Several studies have demonstrated that IPMCs are well suited for use as soft actuators for bending and sensing.[35–37] Potential applications include mechanical grippers, metering valves, micropumps, and sensors.[1,30,38] Eamax, Japan has developed a commercially available fish robot that uses IPMC actuators.[39] Due to the low strains and the nature of their actuation their applications for artificial muscle may be limited.

Ionic Gels

Ionic polymer gels consist of a crosslinked polymer, typically a polyacrylic gel acid, in an electrolyte solution. These materials are a class of hydrogels, a type of network polymer that swells in water. Hydrogels have been of interest for use as actuators for some time.[40–43] A hydrogel placed into an aqueous solution can change in shape and volume by a change in the polymer–liquid interaction, and hence the degree of swelling. This change can be brought about by a number of stimuli, the most commonly used is a change in pH. Polyacrylic gel acids will ionize in response to an increase in the pH, causing them to swell.[44] The change

Macromol. Rapid Commun. **2010**, *31*, 10–36

Macromolecular Journals

DOI: 10.1002/marc.200900425

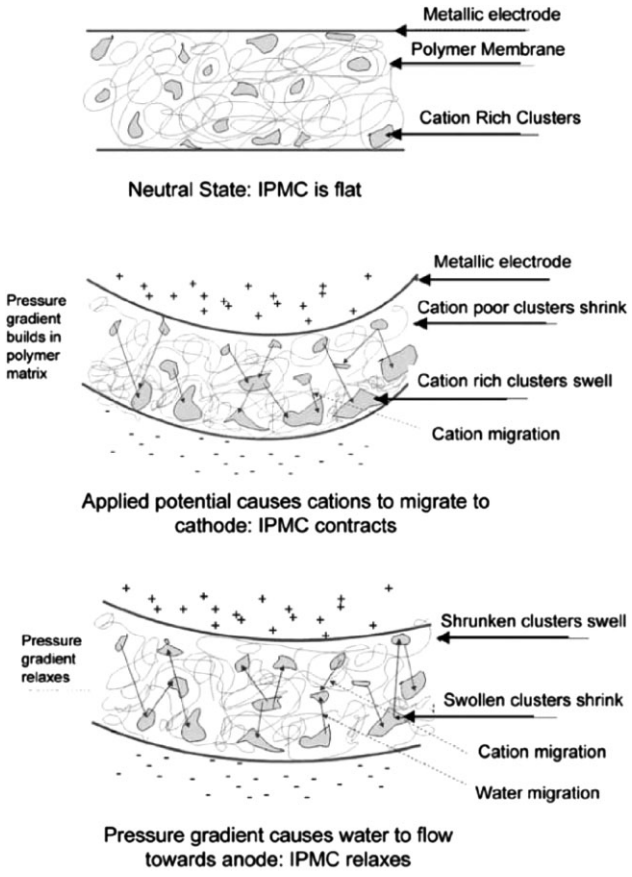

Figure 1. Schematic representation of the actuation mechanism for an IPMC actuator. Application of a bias voltage causes mobile ions to migrate to one of the electrodes. The concomitant migration of solvent causes the ion rich region to swell, generating a bending motion. Over time the actuator relaxes due to the built-up pressure gradient.[2]

in pH can be induced by chemical means, however this approach is impractical as it relies on a fluid-pumping system. Ionic gels also respond to electrical fields.[45] Application of an electric field to the gel causes the migration of hydrogen ions out of or into the gel resulting in a change in pH. The change in pH results in a reversible shift between swollen and contracted states. Actuators tend to bend in response to a DC field, which is caused by the difference between ion diffusion rates in the gel and in the electrolyte solution.[46] While bending may be useful for some applications it is not particularly useful for artificial muscle applications. Calvert and Liu[47,48] have reported on the swelling of layered gels, consisting of crosslinked polyacrylamide layers stacked on polyacrylic acid layers. When the pH is decreased to create a basic environment, the polyacrylic acid layers swell strongly, however the polyacrylamide layers do not. The result is that the stacks expand with only marginal bending. Since the actuation depends on the diffusion of ionic species and the presence of a liquid electrolyte, actuation rates tend to be slow and encapsulation is an issue. These materials are still in the exploratory stages as artificial muscles. Recent work by Tondu et al.[49] has probed the possibility of combining ionic gels with McKibben artificial muscles. The intention is to replace the conventional pneumatic system with a chemical actuation mode with the goal of improving the response speed and reducing system complexity.

Carbon Nanotubes

Since their discovery by Iijima,[50] CNTs have garnered a great deal of interest thanks to their intrinsic mechanical and electrical properties and the ability to functionalize them and incorporate them in composite materials. Individual CNTs possess a high tensile modulus near that of diamond (640 GPa) and their tensile strength is thought to be 20–40 GPa, an order of magnitude larger than any other continuous fiber.[51] The mechanical properties of CNT bundles typically used in actuator tests tend to be much lower since they are held together by relatively weak van der Waals forces.[52] CNTs suspended in an electrolyte are capable of expanding in length due to double-layer charge injection.[2] When a bias is applied between the CNTs and a counterelectrode, ions migrate to the surface of the CNTs. The resulting charge build-up must be offset by a rearrangement in the electronic charge within the tubes. The resulting actuation is due to these effects and to Coulombic forces.[2,24] Figure 2 shows a schematic representation of the actuation mechanism. At low charge injections the quantum mechanical charge redistribution effects can predominate while at moderate to high levels the Coulombic effects dominate.[52] This mechanism does not require ion intercalation so lifetime and actuation rate is higher than for most ionic EAPs. CNTs possess low actuation voltages (≈1 V), high operating loads (26 MPa), high effective power to mass ratios of 270 $W \cdot kg^{-1}$, and a response speed in the millisecond range.[53] They should also be capable of work densities per cycle that are higher than any other current actuation material due to their high modulus. Strains are typically $<2\%$[2] since CNTs are stiff and as such they would require strain amplifiers to be used as artificial muscles. Creep is also an issue, and can negatively affect the measured work densities.[54] CNTs also suffer for very poor electromechanical coupling. This can be partly attributed to the disparity in modulus between individual nanotubes and nanotube bundles.[48] Related work on polymer nanofibers has shown that the elastic modulus increases exponentially from bulk materials to nanofibers with diameters in the range of tens of nanometers.[55] Multiwall CNTs tend to have lower strains than single-wall CNTs since they have a lower exposed surface area to capture ions;[2] however Hughes and Spinks[56] have shown that strains in excess

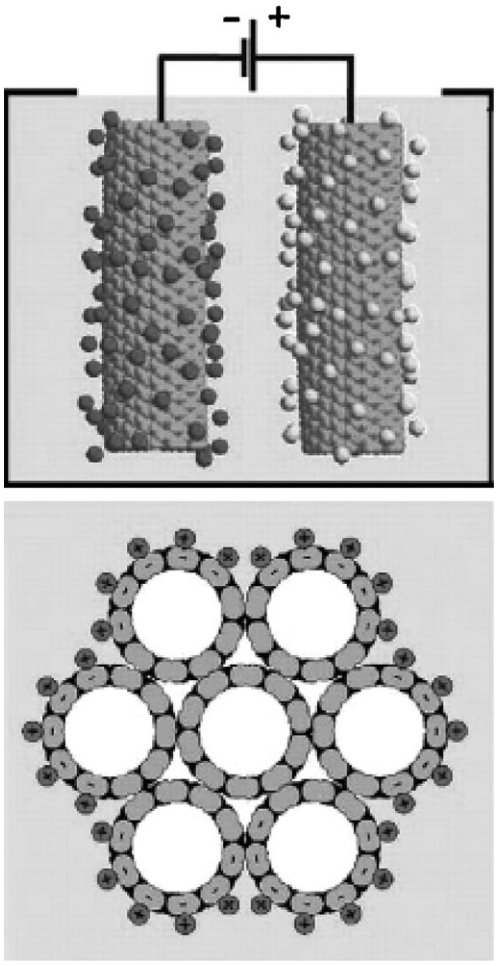

Figure 2. Schematic representation of the actuation mechanism for a CNT actuator. When a bias is applied to CNTs that are submerged in an electrolyte, ions will migrate to the surface of the CNTs, which is offset by the rearrangement in their electronic structure. This phenomenon, coupled with Coulombic effects, results in actuation.[7]

of 0.2% are possible in multiwall CNT mats. Cost and manufacturing difficulties are issues that are currently being addressed.[57,58]

Aliev et al.[59] have recently reported on novel giant-stroke, superelastic CNT aerogel muscles. The CNT aerogel sheets are fabricated from highly ordered CNT forests and are capable of anisotropic linear elongations of 220% and strain rates of 3.7×10^4% s^{-1} at temperatures from 80 to 1900 K. The actuation decreases the aerogel density and the strain can be permanently frozen in. Unlike conventional CNT actuators, no electrolyte is required and the actuation results from applying a positive voltage with respect to a counterelectrode. The actuators have gas-like density and highly anisotropic mechanical properties, with Poisson's ratios reaching 15.

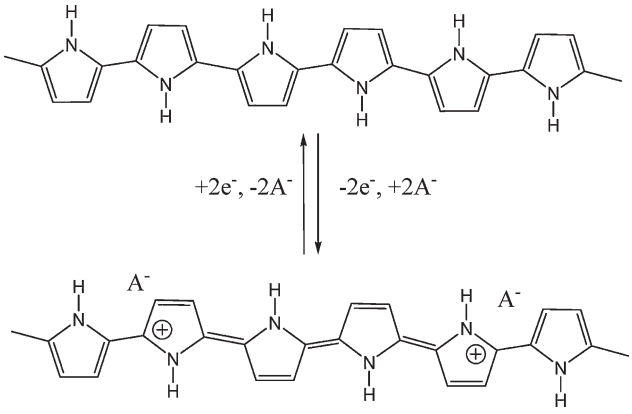

Figure 3. Schematic representation of a polypyrrole chain in its oxidized and reduced states. Actuation results from the intercalation and deintercalation of ions between the chains.

Conductive Polymers

Actuators based on CPs were first proposed by Baughman et al. in 1990.[60–62] Much of the exploratory work was subsequently reported by Pei and Inganäs, Smela and Inganäs, and Otero et al.[63–66] CPs actuate due to the uptake of counterions during electrochemical redox cycling, with the majority of the expansion occurring perpendicular to the polymer chain direction, indicating that ions and solvent are incorporated between the polymer chains.[61,67–69] Changes in oxidation state result in a charge flux along the polymer chain and counterions in the electrolyte migrate to balance the charge.[1,2,7,20,69,70] For polymers doped with moderately sized counteranions, the oxidized state causes the polymer chains to expand due to the presence of the counteranions; in the reduced state the ions migrate away and the polymer chains relax. In polymers doped with bulky counteranions, the reduction involves uptake of cations into the polymer. The reduced polymer is in the expanded state.[69–71] Since both states are stable, these actuators are bistable. The most commonly used CPs for actuation purposes are polypyrrole and polyaniline (PANI).[64,72] Figure 3 shows a schematic representation of a polypyrrole chain in its oxidized and reduced state. Actuation voltages are typically low (1–2 V)[63] and the materials are biocompatible. Strains are typically a few per cent but can range from 1 to ≈40%.[2,7,73–77] Force densities up to 100 MPa are achievable[78] and values up to 450 MPa may be possible.[63] CPs suffer from a very low operating efficiency of ≈1% and electromechanical coupling under 1%.[2] In addition, actuation speeds are limited since the mechanism relies on the migration of ions[20] and due to internal resistance between the electrolyte and polymer.[4] Due to the requirement of an electrolyte, most CP actuators must be encapsulated,[79] though work has been performed on developing solid electrolytes that would remove this restriction.[80] Application of these materials for artificial

Macromol. Rapid Commun. **2010**, *31*, 10–36

Macromolecular Journals
DOI: 10.1002/marc.200900425

muscles may be limited due to their poor coupling efficiencies and relatively slow actuation speeds (which would be exasperated in large devices), though other potential biomimetic and human-interface applications exist that include blood vessel reconnection, dynamic Braille, valves, and catheters.[81–83]

Field Activated EAPS

Ferroelectric Polymers

Ferroelectric polymers have a non-centro-symmetric structure that exhibits permanent electric polarization. These materials possess dipoles that can be aligned in an electric field and maintain their polarization. The induced polarization can be removed by applying a reverse electric field or by heating above the material's Curie temperature. They exhibit nonlinear polarization curves demonstrating pronounced hysteresis. The polymers exhibiting these properties are limited mainly to poly(vinylidene difluoride) (PVDF), some PVDF copolymers, certain odd-numbered polyamides such as Nylon 7 and Nylon 11,[84] and blends thereof.[85,86] In order to display ferroelectric behavior, polymers not only require polar side groups, they must also maintain molecular configurations in which the polarity does not cancel out. Thus, polymers such as poly(vinyl chloride) that has a polar C–Cl bond will not display ferroelectric behavior as it must arrange itself in a helical conformation due to steric effects from the relatively large van der Waals radius of the Cl atoms. Additionally, the polymer chains must be able to crystallize in a manner in which the polarization does not cancel. As an example, PVDF has four crystal structures,[87,88] a non-polar alpha phase, its polar analog (the delta phase), a highly polar beta phase, and a polar gamma phase. The morphology of the crystals must also be considered as they can have pronounced effects on the Curie temperature, remnant polarization, and other properties.

For commonly used poly(vinylidene fluoride trifluoroethylene), or P(VDF–TrFE), copolymers with a VDF content ranging from 50 to 85 mol-%, the ferroelectric beta phase is stable at room temperature, and a transformation to the paraelectric alpha phase occurs above the Curie point but below the melting point.[89] Above the Curie temperature a transition between the paraelectric and ferroelectric phases can be brought about by applying an electric field.[90,91] The change in phases results in an extremely large change in lattice constant resulting in large bulk strains.[92] The Curie point decreases with decreasing crystallite size and can also be influenced by mechanical stress.[18] The induced change between the ferroelectric beta phase and paraelectric alpha phase is represented schematically in Figure 4.

These materials have shown piezoelectric responses after appropriate poling.[18] Their piezoelectric actuation properties are typically worse than ceramic piezoelectric crystals, however they have the advantages of being lightweight, flexible, easily formed, and are not brittle. Additionally, while ceramics are limited to strains on the order of 0.1%, ferroelectric polymers are capable of strains of 10%[91] and very high electromechanical coupling efficiencies.[93]

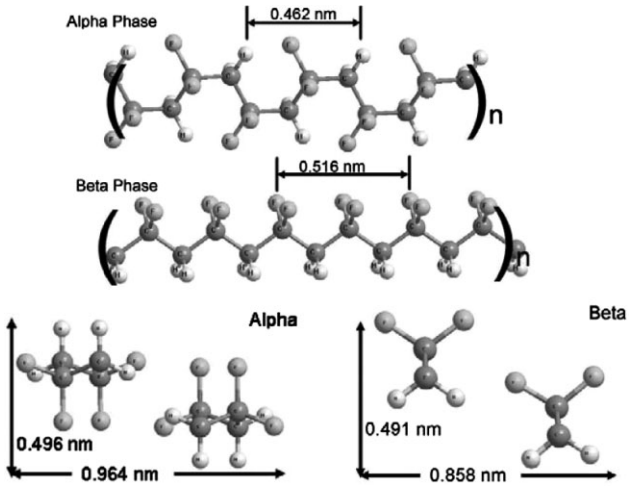

Figure 4. The alpha and beta phases of the ferroelectric polymer PVDF. The beta phase is stable at room temperature but can be reversibly changed to the alpha phase by heating above the Curie temperature. Above the Curie temperature, an electric field can be used to induce a change between the alpha and beta phases. For ferroelectric relaxor polymers, the Curie temperature is below room temperature so the alpha phase is stable. A change to the beta phase can be induced by an electric field.[7]

Recent advances in PVDF-based materials have led to the elimination of the hysteretic behavior characteristic of ferroelectrics, for this reason these PVDF-based materials are classified as relaxor ferroelectric polymers; they will be discussed under the Electrostrictive Polymers Section.

Polymer Electrets

Early work by Eguchi on wax electrets[94] paved the way for the development of commercially viable low cost polymer electrets, with applications including microphones, sensors, transducers, and filters.[18] Electrets are insulating materials that display piezoelectric effects due to a non-uniform space charge distribution.[95,96] Modern polymer electrets consist of a highly porous polymer with a polarization gas in the pores. The porous films are subjected to corona charging with voltages ranging from 5 to 10 kV. It is generally accepted that electrical discharging within the pores results in the build-up of charges at the polymer–gas interface. Positive and negative charges will lie on opposite sides of the pores according to the direction of the applied field, forming macroscopic dipoles.[18] Metal electrodes are applied to both sides of the film to act as contacts.

Polymer electrets can be operated as sensors or actuators. Their operation is very similar to that of a piezoelectric

material and their direct piezoelectric transducer coefficient (d_{33}) is higher than that of solid PVDF ferroelectric polymers.[97] If a compressive force is applied to the film, the pores will deform preferentially with respect to the polymer material. Unlike charges within the polymer will be pushed closer together and the potential measured at the contacts will change accordingly. Similarly, the application of a voltage across the electrodes will yield a change in thickness in the material.

In order to meet increasing performance demands for electret applications, polymer electret blends are being explored. Lovera et al.[98] have recently reported on tailored polymer electrets based on poly(2,6-dimethyl-1,4-phenylene ether) (PPE) and its blends with PS. They obtained good electret performance with neat PPE and showed that it could be improved by blending with PS.

Electrostrictive Polymers

Electrostrictive polymers have a spontaneous electric polarization. Electrostriction results from the change in dipole density of the material. These polymers contain molecular or nanocrystalline polarizations that align with an applied electric field. PVDF copolymers with nanosized crystalline domains, electrostrictive graft copolymers, and liquid crystal elastomers (LCEs) fall under this category.

Relaxor Ferroelectric Polymers

Relaxor ferroelectric polymers are intimately related to the ferroelectric polymers described above. All known relaxor ferroelectric polymers are based on the P(VDF–TrFE) copolymer. As the name suggests, these polymers behave as relaxor ferroelectrics, which are distinguished by a broad peak in dielectric constant and a strong frequency dispersion.[99,100] Two of the major limitations of the P(VDF)-based ferroelectric actuators are that the electrically induced paraelectric–ferroelectric transition that allows for actuation only occurs at temperatures above the Curie temperature, which is usually above room temperature, and the existence of strong hysteresis that can make actuation more energy intensive and difficult to control. The Curie temperature of P(VDF–TrFE) copolymers can be lowered by introducing defects into the material, thereby reducing the size of the crystallites in the solid PVDF copolymer.[18] Having smaller crystallites also lowers the energy barrier required for the transition between paraelectric and ferroelectric states, which results in lower hysteresis.[101] For efficient room temperature operation, the Curie temperature must be reduced to around room temperature and the hysteresis must be suppressed. Zhang and others have shown this can be achieved by irradiating P(VDF–TrFE) with high-energy electrons or protons[101–104] or adding bulky side groups to the copolymer,[102,105–107] thus introducing polarization defects that destabilize the ferroelectric phase. Bulky side groups can be introduced though the formation of copolymers containing PVDF, TrFE, and either chloride containing monomers such as cholorofluoroethylene (CFE)[102,105] and chlorotrifluoroethylene (CTFE)[106,107] or hexafluoropropylene (HFP).[108–110] The actuation mechanism is essentially the same as for ferroelectric polymers; a transition between paraelectric and ferroelectric phases is induced by the application of a high electric field as represented in Figure 4.

Recent work by Bao et al.[111] has shown that P(VDF–TrFE) synthesized via reductive dechlorination from P(VDF–CTFE) exhibits ferroelectric relaxor behavior at high temperature (≈100 °C) with a melting point near 200 °C. This result is important as it provides another avenue to study the relaxor phenomena which is still not completely understood. The high melting point coupled with the high dielectric response of these materials at high temperature makes them attractive for use in high-temperature capacitors.

These materials have shown thickness strains on the order of 5% with fast response times.[18] Representative results are shown in Figure 5. As seen in the figure, the required fields are quite high as in most electronic EAPs. Strains tend to show a peak and decrease for stresses above and below the peak value. Reported values for irradiated P(VDF–TrFE) show peak strains at 20 MPa, dropping to 50% of the maximum value above 40 MPa and below 5 MPa.[112] Elastic moduli in the range of 0.3–1.2 GPa have been reported with energy densities around 1 MJ · m^{-3}.[7] In order to compete as artificial muscles, strain values will have to be improved.

Electrostrictive Graft-Copolymers

Electrostriction has also been obtained from graft copolymers wherein polar crystallites are grafted to flexible polymer backbones. The polar side groups aggregate to form crystalline regions which serve as the polarizable moieties required for actuation and as physical crosslinking

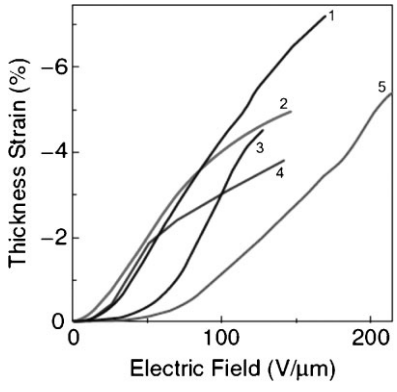

Figure 5. Actuation strain as a function of electric field for irradiated P(VDF-TrFE) copolymer (2), P(VDF-TrFE-CTFE) (4), P(VDF-CTFE) (5) and P(VDF-TrFE-CFE) (1 and 3, the two curves have different compositions).[18]

Macromol. Rapid Commun. **2010**, *31*, 10–36

Macromolecular Journals
DOI: 10.1002/marc.200900425

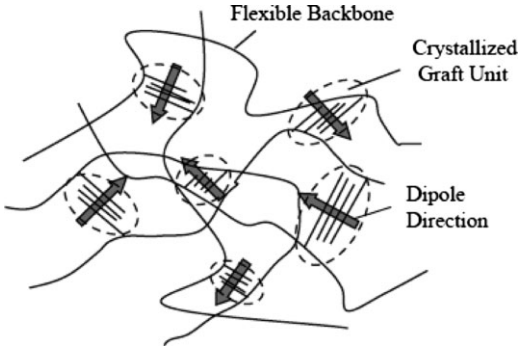

Figure 6. Electrostrictive graft copolymer consisting of P(VDF–TrFE) main chains and PVDF grafts. Polar aggregate and form crystallites that serve as polarizable moieties for actuation and as physical crosslinks between elastomer chains.[113]

sites for the flexible polymer as shown schematically in Figure 6.[113] When an electric field is applied to the copolymers, the polar crystallites reorient themselves which results in bulk deformation of the material. Strains and energy densities can be as high as 4% and 247 $J \cdot kg^{-1}$.[114] Similar results have been reported for a graft copolymer consisting of chlorofluoroethylene and trifluoroethylene backbone with P(VDF–TrFE) side chains.[1] While the required electric fields are lower than for relaxor ferroelectrics, the strains are lower and the actuation rates are slower due to the size of the polar crystallites. Unimorph and bimorph bending actuators have been demonstrated.[114]

Liquid Crystal Elastomers

As the name suggests, LCEs combine the orientational ordering properties of liquid crystals with the elastic properties of elastomer networks.[115] As early as 1975, de Gennes et al.[116] predicted that the reorientation of mesogens in liquid crystals during a phase transition could result in bulk stresses and strains. LCEs were first proposed for use as artificial muscles by de Gennes[117] in the late 1990s. LCEs consist of mesogens attached to one another via a networked elastic polymer. The polymer network permits sufficient motion to allow for the rotation of the mesogens while maintaining a solid shape and preventing free flow. LCEs can be divided into two categories depending on the phases present: nematic and smectic. The actuation mechanism for these two systems is different. Here we will briefly describe the nematic system since it is the focus of the majority of the current research in the field; the interested reader can consult ref.[118–120] and ref.[121] for a detailed look at the nematic and smectic systems respectively. In nematic polymer systems where the mesogens are incorporated directly into the backbone the chains will elongate in their nematic phase when all of the mesogens are aligned[122–124] and will relax when the polymer is in the isotropic state and the chains are allowed to coil up into their entropically favored positions.[125] Similar effects are observed when the mesogens are attached as grafts to the elastomeric backbone. The change in orientation can be effected via thermal and electrical stimuli.[116,118,121,126–132] Thermally activated LCEs display length changes as high as 400% but their response speed is limited due to the requirement for heat diffusion.[117,133,134] Several strategies have been investigated for improving the thermal diffusivity[129,135] of LCEs but thermal relaxation is still an issue. The thermal response can be generated from a number of stimuli including optical, electrical, and direct magnetic through the incorporation of appropriate additives.[136] Electrically activated LCEs have intrinsically polarized mesogens that can realign in the presence of an electric field to generate bulk stress and strain as shown schematically in Figure 7.[116] Electrically activated LCEs have much faster response speeds (10 ms)[121] than the thermally activated variety and the required fields (1.5–25 $MV \cdot m^{-1}$) are lower than for most other field activated EAP technologies; however, the actuation strains are relatively small (<10%). Recent results have shown 4% strain at 133 Hz with a field strength of 1.5 $MV \cdot m^{-1}$.[121] The combination of small to moderate strains with low moduli means that the work densities of these materials will be relatively low. The use of stiffer polymers yielded strains of 2% at 25 $MV \cdot m^{-1}$ and a work density of

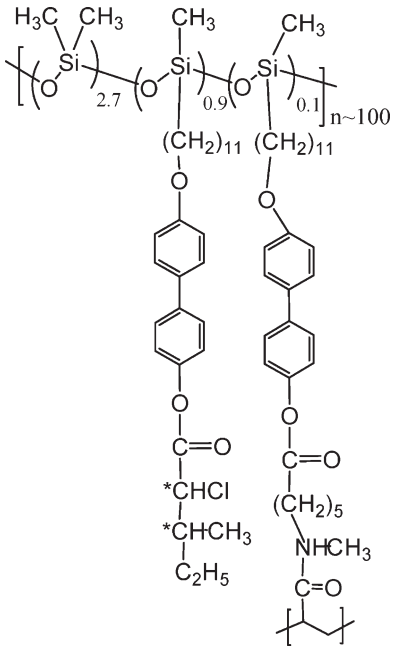

Figure 7. Chemical structure of a liquid crystal elastomer and its actuation mechanism. The application of an electric field results in the realignment of intrinsically polarized liquid crystal mesogens. The mesogens are either grafted to elastomer chains or incorporated within them. The elastomer chains prevent the free flow of the mesogens and couple their motion to bulk stresses and strain (adapted from Lehmann et al.[121]).

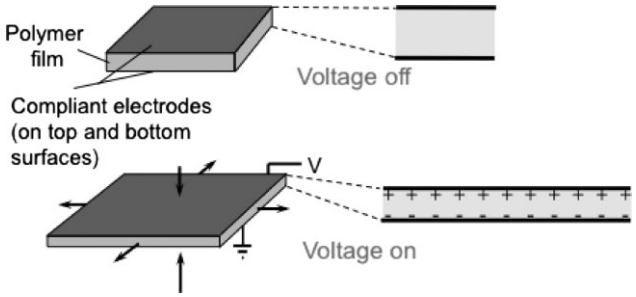

Figure 8. Dielectric elastomer (DE) operating principle. When a bias voltage is applied across an elastomer film coated on both sides with compliant electrodes, Coulombic forces act to compress the film in the thickness direction and expand it in plane.[1]

$0.02\ MJ \cdot m^{-3}$.[131] Additional improvements in strain and work density will be required if LCEs are to compete as artificial muscles. Recent results have shown that the application of a high electric field across a smectic LCE results in a large electroclinic effect with reasonable rates at relatively low voltages that can be used for actuation.[137,138]

Dielectric Elastomers

DE actuators are essentially compliant variable capacitors. They consist of a thin elastomeric film coated on both sides with compliant electrodes. When an electric field is applied across the electrodes, the electrostatic attraction between the opposite charges on opposing electrode and the repulsion of the like charges on each electrode generate stress on the film causing it to contract in thickness and expand in area (Figure 8). Most elastomers used are essentially incompressible, so any decrease in thickness results in a concomitant increase in the planar area.

Typical operating voltages for DE films 10–100 μm in thickness range from 500 V to 10 kV. The area expansion can be readily measured if the films are subjected to tensile prestrain: the non-active areas in tension surrounding the active area pulls the expanded active area and keeps it flat (Figure 9).

The driving currents are very low and the device is electrostatic in nature, so it will theoretically only consume power during an active area expansion (thickness reduction) and no power will be consumed to maintain the DE at a stable actuated state. Furthermore, some of the energy can be recovered after the actuation cycle is complete. In practice, however, there will be some leakage current through the dielectric, the amount of which will depend on the material and its thickness, and thus the DE will consume a small amount of power when maintained in a stable actuation state. Viscoelastic effects may also play a role in reducing efficiency.

Output stress varies quadratically with electric field, however, due to the inherent compliance of the materials, the force that can be coupled to a load will decrease with increasing strain for a particular electric field. Maximum force is available at zero strain and at maximum strain the elastomer will not generate any output forces. Note also that for a given strain the output force, and thus the stiffness, can be modulated by varying the applied field. This is an important feature for artificial muscle applications as it allows the DE actuators to "brace" themselves as natural muscles do to maintain stability or prevent damage.

Modeling of DE Materials

The actuation of DEs can be approximated as the lateral electrostatic compression and planar expansion of an incompressible linearly elastic material where the electrical component is treated as a parallel plate capacitor.[139] The incompressibility constraint can be expressed as

$$Az = P \tag{1}$$

Where A is the area of the electrodes, z is the thickness of the elastomer film between electrodes, and P is a constant. The stored electrical energy on the DE is given by the stored energy on a parallel plate capacitor

$$U = 0.5\frac{Q^2}{C} = 0.5\frac{Q^2 z}{\varepsilon_r \varepsilon_0 A} \tag{2}$$

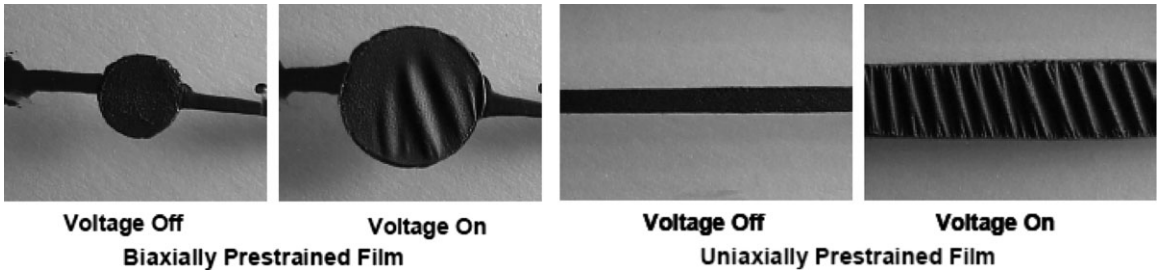

Figure 9. Actuation of DE devices with biaxial and uniaxial prestrain. Uniaxial prestrain results in preferential in-plane strain in the direction perpendicular to the applied prestrain direction.[1]

Macromol. Rapid Commun. **2010**, *31*, 10–36

Macromolecular Journals
DOI: 10.1002/marc.200900425

where Q is the charge on the electrodes, C is the capacitance, ε_r is the relative permittivity, and ε_0 is the permittivity of free space. The electrostatic pressure across the electrodes is then given by the Maxwell pressure

$$p = \varepsilon_r \varepsilon_0 E^2 \tag{3}$$

This is exactly twice the pressure across a parallel plate capacitor. The factor of two is due to the incompressibility of the elastomer film. Charges on opposite electrodes will attract one another, resulting in a reduction in thickness as well as a concomitant increase in area since the material is incompressible. Likewise, like charges on each electrode will also repel each other causing an increase in area and a concomitant reduction in thickness.

Using the linear-elasticity and free boundary approximations used in the early work in the field, which is only valid for small strains (<10%), the change in thickness is given by[139]

$$s_z = -\frac{p}{Y} = -\frac{\varepsilon_r \varepsilon_0 E^2}{Y} = -\frac{\varepsilon_r \varepsilon_0 (V/z)^2}{Y} \tag{4}$$

where V is the applied voltage and Y is the elastic modulus.

Krakovsky et al.[140] provide a good derivation of this linear small-strain case and extended these derivations to include the effects of electrostriction that may be important for certain materials. Pelrine et al.[3,141] showed that for the small strain case, the actuator energy density is given by

$$e_a = -ps_z = \frac{(\varepsilon_r \varepsilon_0)^2 E^4}{Y} = \frac{(\varepsilon_r \varepsilon_0)^2 (V/z)^4}{Y} \tag{5}$$

This equation considers that both the expansion and contraction in an actuation cycle can exert work. Similarly, the elastic energy density is given by

$$e_e = -\frac{1}{2} ps_z = \frac{1}{2} \frac{(\varepsilon_r \varepsilon_0)^2 E^4}{Y} = \frac{1}{2} \frac{(\varepsilon_r \varepsilon_0)^2 (V/z)^4}{Y} \tag{6}$$

For larger strains, while maintaining the assumption that the material is linearly elastic, they showed that[139]

$$s_z = \frac{2}{3} + \frac{1}{3}\left[f(s_{z0}) + \frac{1}{f(s_{z0})}\right] \tag{7}$$

where

$$f(s_{z0}) = \left[2 + 27 s_{z0} + \frac{[-4 + (2 + 27 s_{z0})^2]^{1/2}}{2}\right]^{1/3} \tag{8}$$

and

$$s_{z0} = -\varepsilon_r \varepsilon_0 \frac{V^2}{Y z_0^2} \tag{9}$$

In this case, the elastic energy density is[3,141]

$$e_e = Y[s_z - \ln(1 + s_z)] \tag{10}$$

The preceding equations provided a reasonable foundation for predicting DE behavior, indeed the assumption that DEs behave electronically as variable parallel plate capacitors still holds; however, the assumptions of small strains and linear elasticity limit the accuracy of this simple model. More advanced nonlinear models have since been developed employing hyperelasticity models such as the Ogden model,[142–145] Yeoh model,[145,146] Mooney–Rivlin model,[143,144,147,148] and others (Figure 10).[145,149,150] Models taking into account the time-dependent viscoelastic nature of the elastomer films,[146,148,149] the leakage current through the film,[149] as well as mechanical hysteresis[151] have also been developed.

Recently Zhao and Suo[152] developed a thermodynamic model of electrostriction for elastomers capable of large deformation that helps elucidate the roles that different electrostrictive effects play at different strain levels. Others have attempted to study dynamic effects for actuators subjected to time-varying voltage and pressure inputs.[153,154]

Models have been used to study the failure modes and instabilities present in DEs, including the thermodynamic electromechanical instability (pull-in),[155–161] wrinkling/buckling,[156,157] mechanical rupture,[157,158] and dielectric breakdown[157,158] for select actuator configurations. An improved understanding of these failure modes should allow for the design of actuators capable of operating in a safe regime, thus prolonging actuator lifetime.

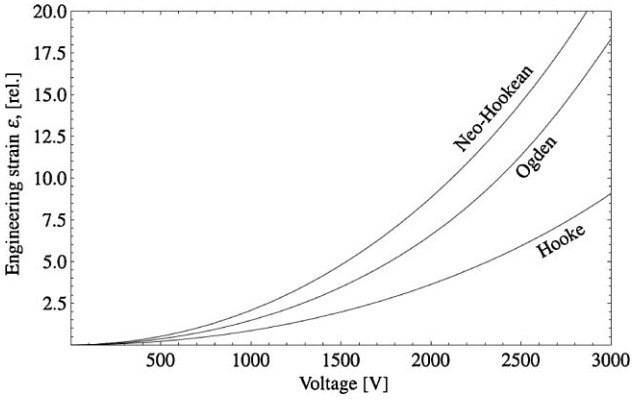

Figure 10. DE voltage–strain curves as predicted by various models.[145]

The applicability of any of the models to a general case is suspect since the modeling parameters are strongly dependent on the testing conditions. Factors such as prestrain, mechanical loading, actuator configuration, humidity, and temperature can have a large effect on the parameters obtained. However, these studies have provided useful insight into the failure mechanisms present in DE actuators and provide tools for design engineers to develop new actuator configurations capable of large strains, high forces outputs, and long lifetimes.

DE Materials

In the late 1990s and early 2000s a large number of elastomer materials were tested, including silicones, polyurethanes (PUs), isoprene, and fluoroelastomers.[139,140,162,163] Pertinent properties of these materials and several other DEs described below are included in Table 2. Pelrine et al. identified three particularly promising groups of materials: silicones, PUs, and acrylics. Their actuation characteristics were promising; however, it was not until strains in excess of 100% in area in both silicone and acrylic elastomer films was reported that significant interest was garnered in the scientific community.[141,164] The key to developing such large strains in these materials was prestrain. Though the exact mechanism by which actuation strains are improved is not known, it has been shown that prestrain enhances the breakdown field in certain acrylic elastomers and can reduce viscoelastic effects.

Of these materials, a commercially available 3M VHB acrylic elastomer (VHB 4910 and VHB 4905) appears to be the most promising in terms of strain performance, with strains in excess of 380% reported for highly prestrained films.[4] The theoretical energy density of this elastomer is an impressive 3.4 $MJ \cdot m^{-3}$ and coupling coefficients as well as efficiencies as high as 90% are possible.

PU films were pursued because of their larger force outputs and higher dielectric constant, allowing them to be actuated at lower electric fields. However, PU films are limited in their ability to generate large strain.

Silicone elastomers have the advantage of lower viscoelasticity than acrylic films and can therefore be operated at higher frequencies with lower losses. Silicones show modest actuation strain when there is little to no prestrain and can be operated over a wide temperature range making them more suitable to applications where temperatures are expected to vary significantly. They are also capable of strains in excess of 100% when prestrained but fall short of acrylics in this area. Silicones also possess a relatively low dielectric constant and thus require higher electric fields.

Carpi et al.[165] have reported on the actuation characteristics of another commercially available elastomer (Dr. Scholl's, Canada, Gelactiv tubing). The material was capable of thickness strains of 1.8% at 27 $MV \cdot m^{-1}$ with an actuation stress of 3.7 kPa at 24 $MV \cdot m^{-1}$.

It follows that many of the most exciting DE materials were discovered via exploratory testing. New formulations of commercially available elastomers are continually being developed and may well be worth exploring. However it is expected that research focusing on developing materials specifically for DE purposes will provide the best candidates for improved performance in the years to come.

Effects of Prestrain

It has been found that prestrain can significantly improve the actuation performance of DE devices.[141,163] The observed improvements have been largely attributed to an increase in the breakdown strength,[166–168] which has been explained via a thermodynamic stability criterion.[169] Prestrain has the additional benefits of improving the mechanical efficiency[170] and response speed of most DEs while causing a marginal decrease in the dielectric constant.[171] Prestrain can also be used to achieve preferential actuation in a certain direction by applying high prestrain in the direction perpendicular to the desired actuation direction and low prestrain along the actuation direction.[141]

The effects of prestrain on the actuation performance of DEs have been widely studied from both a practical as well as theoretical perspective,[141,163,166–181] however the mechanism by which prestrain increases dielectric strength is still not completely understood. It is generally believed that premature DE failure is exacerbated by localized defects introduced during manufacture, processing, or through fatigue. The localized defects act to reduce the local breakdown strength in that area which can lead to localized or permanent device failure. Localized pull-in effects, viscoelastic behavior, and high leakage current can also reduce the usable electric field. It is likely that prestrain prevents pull-in effects. As shown in Figure 11 for a given material, a non-prestrained film will undergo a characteristic rapid increase in stress, then a plateau region, followed by a very steep rise in the stress until the film fails via the breaking of covalent bonds. The actuation stress/strain curve will follow the quadratic curve in the figure. For sufficiently high driving voltages, the reduction in film thickness and increase in electric field intensity form a positive feedback loop and the film will continue to be driven thinner and thinner until the local electric field exceeds the dielectric strength of the film, as indicated by the intersection of the quadratic curve and elastic stress curve. This induces the pull-in effect and possible eventual dielectric breakdown. If the film is prestrained, the origin of

Macromol. Rapid Commun. **2010**, *31*, 10–36

Macromolecular Journals
DOI: 10.1002/marc.200900425

Table 2. Comparison of DE material properties.

Polymer (specific type)	Prestrain (x%, y%)	Energy density	Actuation pressure	Thickness strain	Area strain	Young's modulus	Electric field	Dielectric constant[b]	Dielectric loss factor[b]	Mechanical loss factor[c]	Coupling efficiency k^2	Efficiency[d]	References
		$MJ \cdot m^{-3}$	MPa	%	%	MPa	$MV \cdot m^{-1}$[a]				%	%	
Silicone (Nusil CF19-2186)	–	0.22[e]	1.36[f]	32	–	1	235	2.8	54	–	–	–	[3]
Silicone (Nusil CF19-2186)	(45, 45)	0.75[e]	3	39	64	1.0[g]	350	2.8	6.3	0.005	0.05	79	[141,159]
Silicone (Nusil CF19-2186)	(15, 15)	0.091[e]	0.6	25	33	–	160	2.8	–	–	–	–	[141,164]
Silicone (Nusil CF19-2186)	(100, 0)	0.2[e]	0.8	39	63 (linear)	–	181	2.8	–	–	–	–	[141,164]
Silicone (Dow Corning HS3)	–	0.026[e]	0.13[f]	41	–	0.135	72	2.8	65	–	–	–	[3]
Silicone (Dow Corning HS3)	(68, 68)	0.098[e]	0.3	48	93	0.1[g]	110	2.8	79	0.005	0.05	82	[141,164]
Silicone (Dow Corning HS3)	(14, 14)	0.034[e]	0.13	41	69	–	72	2.8	–	–	–	–	[141,164]
Silicone (Dow Corning HS3)	(280, 0)	0.16[e]	0.4	54	117 (linear)	–	128	2.8	–	–	–	–	[141,164]
Silcone (Dow Corning Sylgard 186)	–	0.082[e]	0.51[f]	32	–	0.7	144	2.8	54	–	–	–	[3]
Polyurethane (Deerfield PT6100S)	–	0.087[e]	1.6[f]	11	–	17	160	7	21	≈0.5	≈0.08 (at 30 Hz)	–	[3,204]
Polyurethane (Estane TPU588)	–	0.0025	0.14	8	–	–	8 (at max. strain)	6	–	–	–	–	[208]
Polyurethane–carbon powder composite (Estane TPU588)	–	0.0043	0.14	12	–	–	8 (at max. strain)	6	–	–	–	–	[208]
Fluorosilicone (dow corning 730)	–	0.0055[e]	0.39[f]	28	–	0.5	80	6.9	48	–	–	–	[3]
Fluoroelastomer (Lauren L143HC)	–	0.0046[e]	0.11[f]	8	–	2.5	32	12.7	15	–	–	–	[3]
Isoprene natural rubber latex	–	0.0059[e]	0.11[f]	11	–	0.85	67	2.7	21	–	–	–	[3]
Dr. Scholl's gelactiv tubing	(140, 0)	–	0.0037	1.8	–	–	28	–	–	–	–	–	[165]
Acrylic (3M VHB)	–	3.4[e]	7.2	79	380	–	–	–	–	–	–	60–80	[4]
Acrylic (3M VHB 4910)	(300, 300)	3.4[e]	7.2	61	158	3.0[g]	412	4.8	90	< 0.005	0.18	80	[141,164]
Acrylic (3M VHB 4910)	(15, 15)	0.022[e]	0.13	29	40	–	55	4.8	–	–	–	–	[141,164]
Acrylic (3M VHB 4910)	(540, 75)	1.36[e]	2.4	68	215 (linear)	–	239	4.8	–	–	–	–	[141,164]
Acrylic (3M VHB 4910)	Nominal	0.0057	–	7	7.5	2.3[h]	17	4.2	14.5	–	–	–	[202]
Acrylic (3M VHB 4905)	Nominal	0.0014	0	11	12.4	2.3[h]	34	4.2	20.9	–	–	–	[202]
SEBS161 (5–30 wt.-% copolymer)	(300, 300)	0.141–0.151	–	62–22	180–30	0.007–0.163	32–133	1.8–2.2	92–53	–	–	–	[202]
SEBS161 (30 wt.-% copolymer)	Nominal	0.013	–	14	16.5	1.3[h]	27	–	28	–	–	–	[202]
SEBS217 (5–30 wt.-% copolymer)	(300, 300)	0.119–0.139	–	71–31	245–47	0.002–0.133	22–98	1.8–2.2	88–40	–	–	–	[201]
SEBS217 (30 wt.-% copolymer)	Nominal	0.013	–	16	18.8	1.1	29	–	28	–	–	–	[202]
SEBS75	Nominal	0.0263 (at 30 wt.-%)	–	16 (at 25 wt.-%)	19 (at 25 wt.-%)	12 (at 30 wt.-%)[h]	29–41	2.08–2.12	29	–	–	–	[202]
ACN rubber	(60, 60)	0.084	0.3	20	–	4	50	14	–	–	–	–	[211]
IPN (VHB 4910 — HDDA)	(0, 0)	–	–	70	233	2.5	300	–	–	–	–	–	[196,198]
IPN (VHB 4905 — TMPTMA)	(0, 0)	0.68	1.51	59.36	146	3.94	265.4	2.43	83.5	–	–	–	[200]
IPN (VHB 4910 — TMPTMA)	(0, 0)	3.5	5.06	74.97	300	4.15	418.05	3.27	93.7	–	–	–	[200]

[a]Breakdown field unless otherwise stated; [b]At 1 kHz; [c]At 80 Hz unless otherwise stated; [d]At 80 Hz; [e]Estimated via calculation; [f]Calculated Maxwell pressure; [g]Effective modulus; [h]Measured in compression.

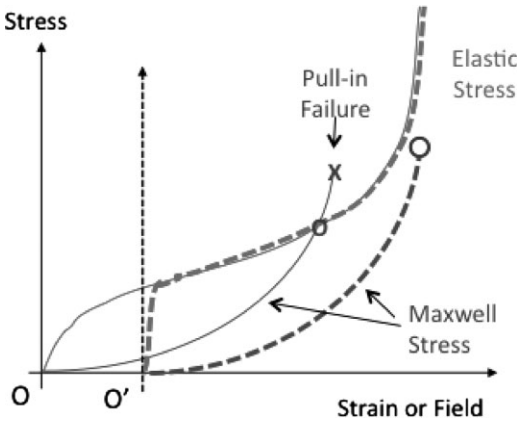

Figure 11. Characteristic stress of a DE film as a function of mechanical strain or electric field (constant voltage condition). The charts with origin at O are for a non-prestrained film and at O' for the prestrained film. The cross (×) indicates dielectric breakdown and the bar (—) indicates stable actuation strain. Small o and large O represent the apparent breakdown field and actual breakdown strength respectively.

the actuation stress/strain curve will shift to O'. The resulting actuation stress/strain curve will be less likely to intersect the elastic stress/strain curve; therefore the actuation will be more stable. Prestrain is very effective for acrylic films and is also effective in silicone and other elastomers; the effect varies from material to material.

Prestrain has the additional benefit of improving the frequency response of many elastomer films. The drop off in actuation strain with frequency is less pronounced for acrylic films that have been prestrained. The increased tension in the film increases the modulus and reduces the viscoelastic nature of the films.

Kofod[182] used advanced materials models in an attempt to elucidate the effects that prestrain has on the actuation performance of a simple cuboid DE actuator. The results are purely phenomenological; however, they indicate that in the special case of a purely isotropic amorphous material prestrain does not affect the electromechanical coupling directly, and that the enhancement in actuation strain due to prestrain occurs through the alteration of the geometrical dimensions of the actuator. He also determined that the presence of an optimum load is related to the plateau region in the force–stretch curve, and that prestrain is not able to affect the location of this region.

The unfortunate drawback to prestraining films is that a rigid frame, or other structure, must be used to maintain the tension in the film. The added mass of the supporting structure increases the total mass of the DE device, which can significantly reduce the effective work density and power to mass ratio of the actuator. The prestrained films may also relax or fatigue over time. This reduces the shelf life of the DE devices.

Improved Silicone Films

A considerable amount of research has focused on reducing the operating voltages of DE actuators in order to increase their commercial viability and remove the dangers associated with high voltage. There are two basic methods of reducing the operating voltage: reducing the thickness of elastomer films so that the required field for high-performance actuation occurs at lower voltages; and increasing the dielectric constant of the elastomer films to reduce the required electric field intensity. Reducing film thickness has the benefit of maintaining the dielectric breakdown strength and dielectric loss of the film but suffers from reduced output force and the increased importance of inhomogeneities that cause localized areas of high electric field and stress and result in premature breakdown. The output force can be scaled up through the use of multilayer actuators but doing so increases fabrication complexity.

A number of approaches have been explored for increasing the dielectric constant of elastomers for DEs. The most common approach involves the addition of high dielectric constant filler materials to an elastomer host. Silicone is of particular interest for this type of approach as it possesses good actuation properties to begin with, is readily available in gel form, and has a low dielectric constant. Results thus far do not appear particularly promising: increases in dielectric constant have been met with concomitant increases in dielectric loss and reductions in dielectric breakdown strength.[183–185] It has also been shown that the elastic modulus is affected by the addition of filler.[186]

Researchers have investigated the effects of adding various oxides including aluminum oxide, titanium oxide, and barium titanium oxide,[185–188] as well as various other fillers including organically modified montmorillonite (OMMT),[189] lead magnesium niobate-lead titanate (PMN-PT),[184,187] copper-phthalocyanine oligomer (CPO),[187,190] and PEDOT/PSS/EG.[191] Improvements appear limited at best as any meaningful increases in the dielectric constant are achieved at loadings near the percolation threshold and are met with increases in the leakage current. Research is still ongoing and some researchers believe that with some additional refinement real improvements can be achieved.

Carpi et al.[192] have recently developed silicone-based polymer blends that display enhanced electromechanical transduction properties. Their technique involves blending, rather than loading, the silicone elastomer with a highly polarizable conjugated polymer. They have reported very promising results for silicones loaded with very low percentages (1–6 wt.-%) of poly(3-hexylthiophene) (PHT). The resulting blends yielded an increase in dielectric permittivity with a relatively small increase in dielectric loss and a reduction in tensile elastic modulus, which

Macromol. Rapid Commun. **2010**, *31*, 10–36

Macromolecular Journals
DOI: 10.1002/marc.200900425

contribute synergistically to an improvement in electromechanical performance. The best performance was obtained for a blend with 1 wt.-% PHT, achieving a transverse strain of 7.6% at a field of only 8 MV · m^{-1}.

Chen et al.[193] have developed an electrothermally actuated CNT–silicone composite. They have been able to produce a maximal strain of 4.4% with an applied field of only 1.5 kV · m^{-1} by incorporating a CNT network into the silicone elastomer. The mechanism of actuation differs strongly from that of conventional DEs. In these materials, the CNT loadings are such that conductivity through the specimen is possible. The flow of current through the CNT matrix causes Joule heating which raises the temperature of the silicone matrix causing it to expand due to thermal effects.

Improved Acrylic Films

Conventional acrylic films, such as the VHB 4910 series of elastomers from 3M, possess excellent actuation strain, energy density, and coupling efficiency. However, in order to achieve these high performance values, the film must be pre-strained. The addition of bulky support frames required to maintain the prestrain on the film significantly increases the mass of VHB acrylic based devices, reducing their effective energy densities to more pedestrian values. VHB acrylic films also suffer from viscoelastic effects which limit their maximum response frequency to the 10–100 Hz range. The viscoelastic nature of these films also limits their overall efficiency and results in time dependent strain that can make their performance somewhat erratic.

Low molecular weight additives can increase the frequency response of VHB films.[194] Representative results are shown in Figure 12. For the film without additives, the strain reduced to half its static value at 12 Hz; for the films with additives this frequency was pushed to over 100 Hz. These additives have the additional benefit of decreasing the glass transition temperature, thereby increasing the range over which the VHB films can be operated. When added in high concentrations, however, the additives reduce the mechanical stability of the films, making them easier to tear.

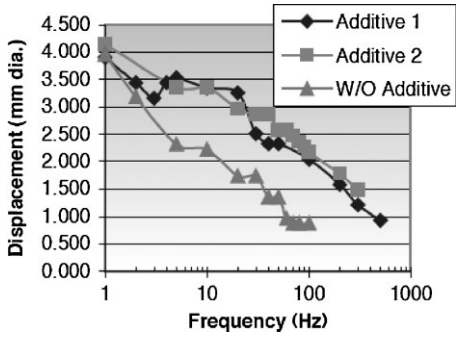

Figure 12. Improved frequency response of VHB acrylic elastomers via the addition of low molecular weight additives (plasticisers).[194]

Interpenetrating polymer networks (IPNs) have been synthesized combining acrylic and silicone rubber materials.[195] These IPN films are synthesized by diffusing silicone chains into swollen acrylic rubber films in the presence of a co-solvent and then crosslinking the silicone chains. The resulting films display properties between those of acrylic and silicone films as expected. Such IPN films provide a simple and easy way to eliminate some of the disadvantages of acrylic films while maintaining high strain performance.

Much more promising results have been obtained in prestrain-locked VHB-based IPNs.[196–200] These IPNs are fabricated by first pre-straining the VHB film to very high strains and spraying a multifunctional monomer onto the film along with an initiator, then allowing the monomer and initiator to diffuse into the film. The additive monomers are then polymerized and form a second network elastomer within the VHB elastomer host. Upon releasing the IPN film from its support, the additive network will resist the contraction of the VHB host, preventing it from returning to its unstrained state. The IPN film will thus remain in a state wherein the VHB film is locked in tension and the additive network is locked in compression. The process is outlined in Figure 13.

The resulting films are capable of performance similar to pre-strained VHB films without the need for a support frame. Ha et al. have reported results for IPNs incorporating bifunctional 1,6-hexandiol diacrylate (HDDA)[196,197] and trifunctional trimethylolpropane trimethacrylate (TMPTMA) monomers.[198,199] With no externally applied prestrain these prestrain-locked IPN films have matched the performance of highly prestrained (300% × 300% biaxial prestrain) VHB4910 acrylic elastomers in terms of strain, electromechanical coupling factor, and energy density.[200] With no externally applied prestrain, the TMPTMA-based IPN films are capable of thickness strains as high as −75%, with an energy density of 3.5 MJ · m^{-3}, pressure of 5.1 MPa, and coupling efficiency of 94%, with a breakdown field of 420 MV · m^{-1}. Figure 14 shows the

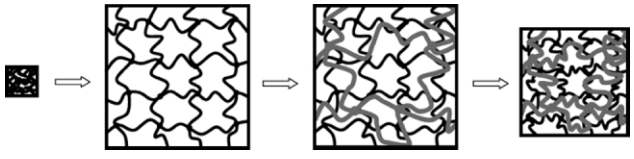

Figure 13. Fabrication steps for IPN elastomer films. The film is first prestrained, and then a multifunctional monomer additive is sprayed onto the host film and polymerized forming an interpenetrating polymer network. Upon releasing the film it retains most of the applied prestrain, with the additive network being in compression and the host film in tension.[199]

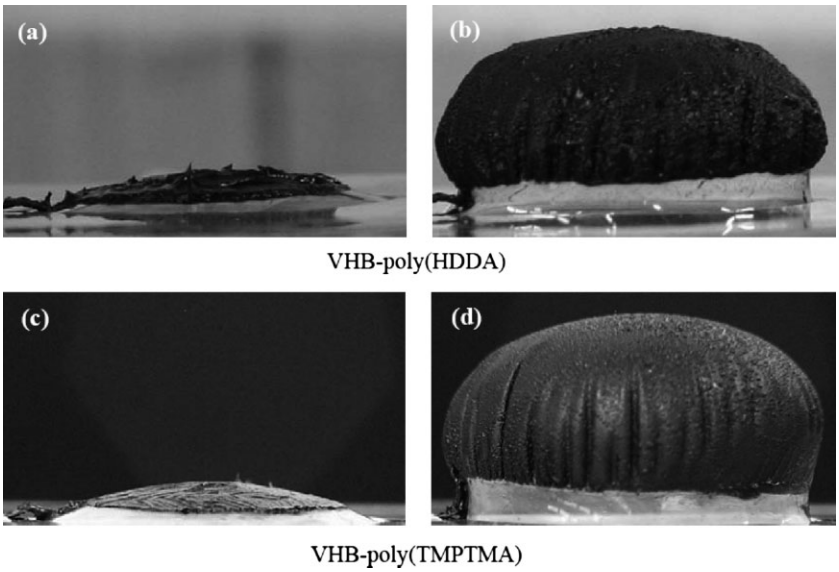

Figure 14. VHB-based IPN films before and after actuation for films with HDDA (a and b) and TMPTMA (c and d) additives in a diaphragm configuration with no externally applied prestrain. Only a small bias pressure was used in the diaphragm chamber as evidenced by the small bulge in the film prior to actuation.

actuation of VHB-based IPN films with HDDA and TMPTMA additives.

IPN films have the added benefits of reducing viscoelasticity and enhancing mechanical stability as compared to regular VHB acrylic elastomers.[200] Reduced viscoelasticity has led to improvements in mechanical efficiency as seen in Figure 15. These materials should open the door to a host of new actuator configurations and applications with minimal supporting structures and very high power-to-mass ratios.

Thermoplastic Polymers

Thermoplastic elastomers are also of interest as DE materials. These polymers differ from conventional elastomers in that they possess physical crosslinks rather than chemical ones. In these polymers flexible elastic chain segments separate rigid segments. The rigid sections act as the binding points between chains while the flexible segments allow for large deformations.

Recently, Shankar et al.[201,202] reported on nanostructured PS-*block*-poly(ethylene-*co*-butylene)-*block*-PS (SEBS) triblock copolymers swollen with a midblock sensitive oil. At relatively high oil concentrations, the thermoplastic elastomer behaves as a physical network where glassy styrene micelles serve as thermally reversible crosslinks. The glassy micelles are linked by rubbery ethylene-*co*-butylene midblocks swollen in the oil, giving the copolymer its elastomeric properties. Figure 16 shows a TEM image of a SEBS copolymer in midblock sensitive oligomeric oil with a concentration of 10 wt.-% polymer; the inset is a depiction of the network linked by the glassy micelles. Actuation strains as high as 245% in area (71% thickness) were reported in highly prestrained actuators, exceeding the maximum reported values for silicone and rivaling those reported for VHB acrylic elastomers.

Thanks to the ability to tune the composition by varying the copolymer molecular weight and the weight fraction of the polymer and oil, materials can be fabricated with tensile moduli ranging from 2 to 163 kPa with actuation strains being the highest for the low modulus variety and decreasing to 30% in area (22% thickness) at the high end. Coupling efficiencies achieved were as high as 92% for low polymer loadings and lower molecular weight (161 $kg \cdot mol^{-1}$) and reduced to ≈40% at high polymer loadings and higher molecular weight (217 $kg \cdot mol^{-1}$).

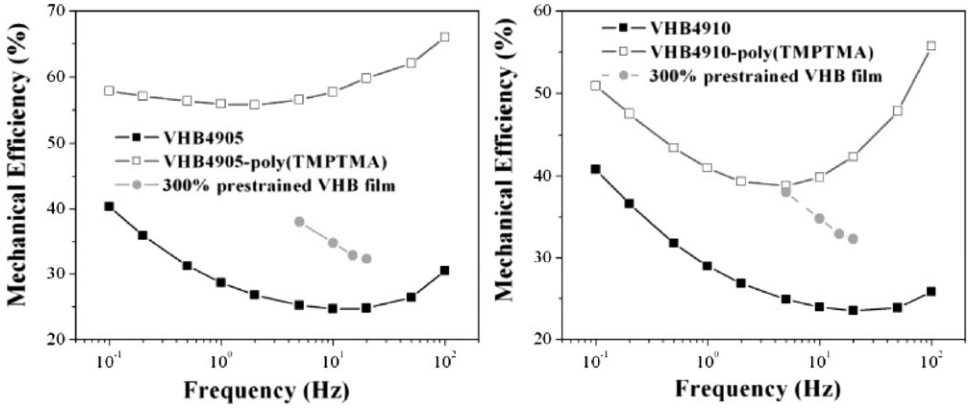

Figure 15. Improved mechanical efficiency for VHB-based IPN films over neat VHB films in both the highly prestrained and un-prestrained states. The improved efficiency over prestrained VHB acrylic elastomers is attributed to a reduction in viscoelasticity.[200]

Macromol. Rapid Commun. **2010**, *31*, 10–36

DOI: 10.1002/marc.200900425

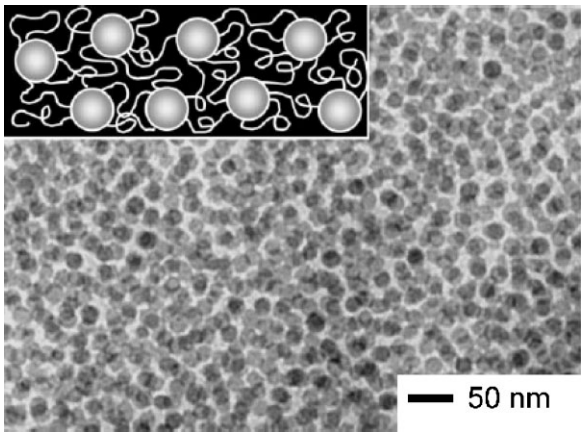

Figure 16. TEM image showing the presence of glassy micelles of an SEBS copolymer in midblock sensitive oil with a polymer loading of 10 wt.-%. The inset is a depiction of the glassy micelle-stabilized polymer network.[201]

A maximum energy density of 289 kJ · m^{-3} was achieved at intermediate polymer weight fractions for the higher molecular weight copolymer. A recent report showed that the materials are capable of blocking stresses as high as 442 kPa with a breakdown field of 203 MV · m^{-1} at a polymer loading of 30 wt.-%.[203] The material also exhibited low cyclic hysteresis. These nanostructured polymers also display favorable actuation characteristics in their non-prestrained state when compared with non-prestrained VHB acrylic elastomers.[202] Unfortunately it appears as though large strains require low polymer loadings, while high blocking stress and breakdown field are limited to higher polymer loadings. The issue is the requirement for a midblock sensitive oil to allow for easier chain movement in the ethylene-*co*-butylene midblocks. Without a high concentration of solvent, the chain mobility is reduced and strains are limited; however, as the concentration is increased the breakdown field suffers and leakage current may increase, limiting the blocking pressure and reducing efficiency. Depending on the solvent used, there may also be leaching issues that can act to degrade the polymer over time.

PU also falls under the class of thermoplastic polymers. The electromechanical response of PU is due to both Maxwell pressure and electrostriction. The Maxwell pressure has been found to have a significant contribution to the strain response of PU films above the glass transition temperature.[204] While PU films initially proved promising, they fell to the sidelines soon after due to the dramatic improvements in the actuation properties of silicone and acrylic films with prestrain. The majority of research since then has focused on PU-based composites. Cameron et al.[205] reported on their findings pertaining to graphite loaded PU films. They reported an increase in the actuation stress by a factor of over 500 and a relative permittivity beyond 4000 for graphite loadings near the percolation threshold. Unfortunately, such high loadings resulted in an increase in the dielectric loss factor by several orders of magnitude and an increase in modulus by a factor of 5. The result was a dramatic increase in the leakage current, power consumption, and a reduction in maximum actuation strain (due to the inability to reach high fields). Nam et al.[206] demonstrated the ability to tune the bulk permittivity and ionic conductivity of PU–montmorillonite (MMT) nanocomposites by varying the gallery heights of the (MMT) nanoplatelets through the addition of different counterions. Resulting permittivity values were shown to vary from below that of pristine PU for both low and high gallery heights, to above the value for intermediate gallery heights, indicative of an optimal gallery height for such composites.

Huang et al.[183] have demonstrated an all-organic three-component PU-based composite with a high electromechanical response. By combining a high dielectric constant copper phthalocyanine oligomer (PolyCuPc) and conductive PANI into a PU matrix they have been able to achieve an electromechanical strain of 9.3% and elastic energy density of 0.4 J · cm^{-3} under an electric field of only 20 MV · m^{-1}. This approach overcomes issues associated with other percolative composites in which the loading of conductive filler must be near the percolation threshold in order to achieve meaningful increases in dielectric constant, which has a deleterious effect on the dielectric breakdown strength of the composite. In the composite, the PolyCuPc enhances the dielectric constant of the PU matrix; the two-component system also acts as the host for the conductive PANI that further enhances the dielectric response via a percolative phenomenon at much lower concentrations than in single component systems. Figure 17 shows the increase in thickness strain achieved in the three-component composite at different filler loadings.

Recent results have been reported on another PU-based composite film.[207,208] A carbon nanopowder was added into a polyether-type thermoplastic (TPU5888 from Estane) at loadings up to 1.5 vol.-%. The maximum thickness strain of the composite was 12% versus 8% in the pure polymer, with a maximum pressure of 0.14 MPa (unchanged), and a response speed in the ms time range under a driving field of 8 MV · m^{-1}. The results may have been limited by the use of sputtered gold electrodes that can contribute to device stiffness and lose conductivity at moderate strains. The energy density of the composite was estimated using FEM simulations to be 4.3 kJ · m^{-3}, a factor of ≈1.7 increase over the pure polymer.

P(VDF–TrFE), a well-studied electrostrictive polymer is also thermoplastic. By dispersing copper–phthalocyanine (CuPc), a high dielectric constant metallorganic compound, into a P(VDF–TrFE) matrix, the resulting composites maintained the flexibility of the matrix with a very high

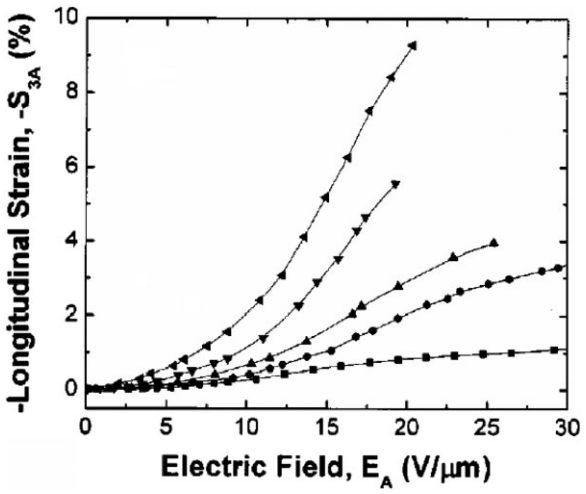

Figure 17. Thickness strain S_{3A} as a function of the applied-field amplitude for composites of PANI/yPolyCuPc/PU (from lowest strain to highest strain): 0:0:100, 0:15:85, 4.6:15:85, 9.3:15:85, 14:15:85.[183]

dielectric constant (425 at 1 Hz) and relatively low dielectric loss.[209] The dielectric constant was shown to vary with both electric field and frequency and was highest at high fields and low frequencies. The strain exhibited a quadratic dependence on electric field, as expected, and a thickness strain of −1.91% was achieved at a field of 13 $MV \cdot m^{-1}$ with an elastic energy density as high as 0.13 $MJ \cdot m^{-3}$. The strain response of the material was attributed to a number of mechanisms, including Maxwell stress and electrostriction.

Other Engineered Elastomers

It is interesting to note that the elastomers that provide the best actuation characteristics (VHB acrylics and silicones) were not designed for use as DEs. Their noteworthy performance is not the result of targeted materials developed, but rather a fortuitous coincidence. The development of new novel engineered DEs has made slow progress; however, in recent years several new developments have been presented that indicate that research is moving toward improved materials with the targeted application of DE actuators for artificial muscle applications.

Jung et al.[210,211] have developed a synthetic elastomer composed of acrylonitrile butadiene rubber copolymer. The properties of the copolymer can be tuned by changing its composition. Reported data for dielectric constant, elastic modulus and strain relaxation are promising (see Table 2). The synthetic elastomer provides some improvement over VHB and some silicone films under certain conditions; however, the tests were limited to low prestrain (60% radial), where the performance of VHB films is poor.

The same group has recently reported on the effects of a plasticizer (dioctyl phthalate — DOP) and a high-K ceramic (TiO_2) on the actuating performance of their synthetic elastomer.[212] The addition of DOP showed the expected results of lower modulus, increased strain, and increased elastic energy density. The addition of TiO_2 had the effect of decreasing the modulus, increasing the dielectric constant, and increasing the strain and elastic energy density up to an optimal value, after which the values were seen to decrease. A maximum energy density of 1.2 $kJ \cdot m^{-3}$ was achieved for a synthetic elastomer with a DOP loading of 100 parts per 100 rubber (phr) with a radial strain of 1.62%. A maximum strain of 3.04% was reported for a DOP loading of 80 phr and a TiO_2 loading of 30 phr. The maximum dielectric constant achieved was 11.1 for DOP and TiO_2 loadings of 80 and 40 phr respectively, but strain and elastic energy density were limited to 1.7% and 0.5 $kJ \cdot m^{-3}$ respectively. The values, albeit lower than the peak performance of most conventional DE materials, were achieved at relatively low electric fields (20 $MV \cdot m^{-1}$ or lower).

Compliant Electrode Materials

Identifying or developing a suitable compliant electrode is also a key factor in achieving good DE performance. A number of electrode materials have been explored. Original tests were performed using thin metal films. While these films provided good electrical conductivity they limited strains to ≈1%. Good compliant electrode materials should maintain high conductivity at large strains, have negligible stiffness, maintain good stability, and be fault tolerant. Common solutions include metallic paints (e.g., silver grease or paint), carbon grease, graphite and carbon powder. Carbon grease electrodes are the most commonly used solution as they provide good conductivity even at very high strains, they are cheap and easy to apply, and they provide good adhesion to most DE materials while having minimal negative impacts on actuation performance. Dry graphite and carbon powder are also cheap, easy to apply, and have the additional benefit of being easy to handle. These dry electrode materials are better suited to multilayer devices where carbon grease electrodes result in slippage between adjacent layers which can eventually result in inhomogeneities in the electrode coverage, however they tend to lose conductivity at high strains as the individual particles are pulled apart and lose contact. A comparative evaluation of some of the early electrode materials was performed by Carpi et al. in 2003.[213]

Improved metal electrodes have been developed by Benslimane et al.[214] The electrodes are capable of achieving an anisotropic planar stain of 33% before losing electrical contact. The key to their design was patterning

Macromol. Rapid Commun. **2010**, *31*, 10–36

Macromolecular Journals
DOI: 10.1002/marc.200900425

the surface of the elastomer itself prior to depositing a layer of silver. The films are able to expand in the corrugated direction, while expansion in the lateral direction is inhibited. Similarly, Lacour et al.[215] achieved 22% strain with gold electrodes by first applying a compressive stress to the elastomer film in order to create surface waves.

Recent studies have been performed on alternative electrode materials. Nanosonic has developed low modulus, highly conducting thin film electrodes by molecular level self-assembly processing methods capable of maintaining conductivity up to strains of 100%.[216,217] Recent developments have enabled the reduction of the modulus to less than 1 MPa and an increase in the strain to rupture to 1000%.[218] A version of the material is commercially available under the name Metal Rubber™. Delille et al.[219] have developed novel compliant electrodes based on a platinum salt reduction. The platinum salt is dispersed into a host elastomer and immersed in a reducing agent. A maximum conductivity of $1\,S \cdot cm^{-1}$ was observed and conductivity was maintained for strains up to 40%.

In order to fully exploit the scalability of DE actuators it necessary to be able to pattern electrodes on the micro scale as well. Rosset el al.[220–223] have explored the use of ion implanted metal electrodes in PDMS. Their results show that conductivity can be maintained for strains up to 175% and can remain conductive over 10^5 cycles at 30% strain. This is of particular importance for MEMS microfluidic devices where the DE microactuators could be used as micropumps. The ion-implanted films maintained high-breakdown fields ($>100\,MV \cdot m^{-1}$) while the Young's modulus increased by 50–200% depending on the dose.

Studies performed by Yuan et al.[224] on conductive PANI nanofibers, P3DOT, and CNT thin films show that all three are capable of forming highly compliant electrodes with fault-tolerant behavior. Nanowires and tubes are of particular interest since they are capable of maintaining a percolation network at large strains, thus reducing the required electrode thickness while still allowing for maximum strain performance.

Further investigations by Lam et al.[225] showed that PANI nanofibers films provided good actuation characteristic, provided fault tolerance, and had a negligible influence on the mechanical properties of the film but lost conductivity over time. When tested on VHB 4905 films prestrained biaxially by 300 × 300% the electrodes provided a maximum area strain of 97% at 3 kV and demonstrated self-clearing with a preserved strain of 91% after the first clearing event.

More recent results on CNTs were much more promising.[226,227] Two types of CNT thin films were tested: functionalized P3-single walled nanotubes (SWNTs) and raw (non-functionalized) SWNTs. Both films provided excellent actuation characteristics (on par with carbon grease), had a negligible influence on mechanical properties of the film, and remained stable over longer periods of time. In addition, the CNT films could be made thin enough to remain optically transparent for use as transparent compliant electrodes.[228]

The ultrathin PANI and CNT thin films are capable of "self-clearing," a process wherein the electrode material is burnt off locally in the event of an electrical short through the dielectric film.[224–227] Dielectric failure is one of the leading causes for premature device failure of DEs and results in terminal failure in carbon grease, graphite, and carbon powder electroded devices. The fault tolerance of devices with CNT electrodes is demonstrated in Figure 18; in the tests a prestrained circular VHB acrylic actuator was punctured with a cactus pin and maintained very high actuation strains. In separate tests, the actuators were driven at a high field until the occurrence of a localized breakdown, the actuators "self-cleared" and recovered well from the local failures and retained high actuation strains. An SEM image of a "self-cleared" region is shown in Figure 19. The image shows that the CNTs in the region surrounding the short have been burnt off. The addition of self-clearing introduces fault tolerance to DEs and can dramatically increase device lifetime. Results for CNT-based electrodes have demonstrated increases in constant actuation lifetime over carbon grease electrode based devices by

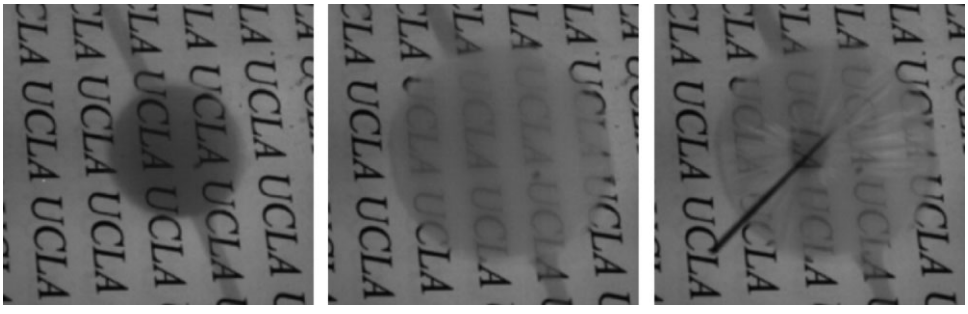

Figure 18. Fault-tolerance of CNT electrodes. DEAs with CNT electrodes are able to withstand puncture and maintain a high level of strain due to self-clearing of CNTs around the puncture. From left to right: prestrained VHB acrylic actuator with CNT electrodes; actuated; actuated with a cactus pin through the active area.[227]

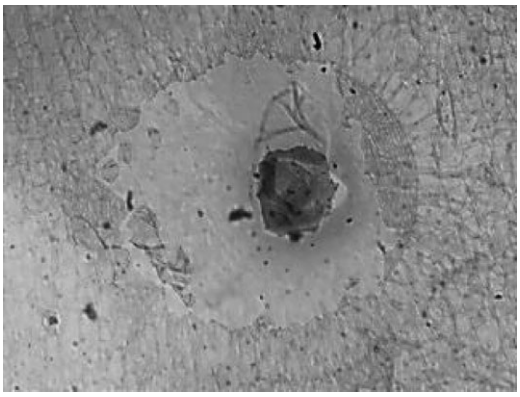

Figure 19. Cleared area on a CNT electrode. Localized dielectric breakdown results in an electrical short through the film. Corona discharging burns away the CNTs in the area surrounding the short, isolating it from the rest of the electrode and allowing the device to continue operating.

two orders of magnitude; they have also demonstrated the ability to withstand and recover from several localized dielectric breakdown events.

Further increases in operational lifetime have been achieved through the addition of a thin layer of dielectric oil over the CNT electrodes.[229] Due to the high field amplification at the CNT tips, corona discharging through the air is an issue. In P3-SWNT films this results in a slow degradation of the electrode conductivity resulting in lower actuation strains over time. Raw-SWNT films suffer from unabated breakdown-clearing events, which persist until the film loses mechanical stability and fails. The dielectric oil fills in the gaps between adjacent nanotube tips and flows into the voids left behind after the clearing events, turning the corona discharging process into silent discharge. This results in fewer breakdown-clearing events and can prolong constant-actuation life at high strains by over an order of magnitude.

With the improved fault tolerance and lifetime afforded by compliant CNT electrodes with dielectric oil, DE artificial muscle devices that are capable of providing high-performance actuation reliably over an extended number of cycles should be possible and should push DE actuators and artificial muscles closer to commercialization.

DE Actuator Configurations

Because DEs are fabricated from conformable elastomers, they can be shaped into many actuator configurations over a wide range of dimensions. Most actuator designs use the area expansion of the DE film for actuation, however, multilayer stacked actuators exist wherein actuation is through a reduction in thickness. Typical designs incorporate support structures to maintain prestrain in the films, though materials and processing advances have allowed for frameless designs as well. The majority of the actuator configurations in use today were developed by SRI in the late 1990s early 2000s.[155,162,230,231] These include rolled (spring and core free), tube, unimorph, bimorph, stretched-frame, diaphragm, bowtie, spider, and extender. Carpi et al.[232] provide a detailed account of DE technology with an emphasis on actuator configurations and applications.

A number of other actuator configurations have been developed, including a bidirectional framed actuator,[233] a multi-degree-of-freedom double diaphragm-type actuator,[234] a tube-spring actuator (TSA),[235] a reinforced cylindrical actuator,[236] an active shell-based actuator,[237] a cone actuator,[238] a compound structure frame actuator,[239] an inflated bending actuator,[240] and thickness mode actuators that can be used in programmable deformable surfaces.[241] Additional efforts have been put into characterizing and modeling the performance of different actuator configurations.[242]

Yet another interesting DE actuator configuration, dubbed DEMES, which stands for DE minimum energy structure, has been introduced by Kofod et al.[243,244] and further developed by O'Brien et al.[245] This type of actuator relies on a thin bendable frame. The frames are designed such that, when a prestrained DE layer is fixed to the frame, the forces exerted by the prestrained DE layer will cause the frame to curl until the forces balance; the result is that the device is curved in the equilibrium rest state. Upon actuation the DE layer will relax causing the actuator to uncurl until it reaches the equilibrium actuated state, which will vary with the applied field.

Plante et al.[246] proposed using bistable binary actuator systems. These actuators are capable of transitioning between two stable rest states and thus do need to be actuated continuously for extended periods of time, which can dramatically improve overall lifetime.

Artificial muscle incorporated (AMI) has developed a universal muscle actuator (UMA) that has been proposed for use as an auto-focusing lens for camera phones.[247] This design relies on coupled prestrained circular framed actuators linked antagonistically and mechanically biased; they are spaced apart around the outer edge and connected at the center. Actuation of one of the films allows the other to relax, resulting in out-of-plane linear displacements.

From the perspective of artificial muscle design, the two most interesting device designs are the spring roll and stacked actuator. Both of them are able to effectively couple the deformations of DEs to provide linear actuation. Spring rolls are interesting from the perspective that they are capable of providing a combination of large linear strains (≈30% of the active area) with relatively large output forces (≈21 N for a cylindrical device measuring 65 mm in length and 12 mm in diameter).[248,249] The main drawback of spring roll actuators is that their design requires several passive or semi-active components such as a compression

Macromol. Rapid Commun. **2010**, *31*, 10–36

Macromolecular Journals
DOI: 10.1002/marc.200900425

Figure 20. Spring roll DEA. Rolls are fabricated by compressing a spring between two endcaps and rolling a DE/electrode/DE/electrode layered strip around it. Increasing the number of layers wrapped around the spring core increases the output force.[251]

spring and end caps. A spring roll actuator can be seen in Figure 20 along with a schematic of the components. A DE/electrode/DE/electrode layered film strip is rolled around a spring compressed between two end caps. When released, the spring acts to maintain the prestrain in the film and prevent buckling. Reliability is an issue as the spring and end caps may generate areas of localized high stress that may result in premature failure.

Spring rolls capable of both bending and elongation have been reported by Pei et al.[250–252] Bending is achieved by patterning the electrodes; for two and three degree-of-freedom actuators two and three electrically isolated electrode pairs are required respectively. By actuating one electrode pair, only a portion of the actuator will elongate, causing the actuator to bend. These actuators are capable of bending angles as high as 90 degrees with lateral forces higher than 1.5 N for cylindrical devices measuring 9 cm in length and 2.3 cm in diameter. The ability to both bend and elongate opens up a number of new possibilities for multidegree of freedom spring rolls. These will be explored in the next section.

Stacked and folded configurations consist of tens to thousands of DE films stacked together and utilize the reduction in thickness rather than the area expansion of the DE film as the means of actuation. Employing a large number of layers amplifies the displacements. Several configurations have been proposed and tested.[253–258] The simplest device consists of laminated layers of DEs sandwiching compliant electrodes. Several silicone-based actuators have been developed and have demonstrated linear strains in excess of 15%.

To reduce manufacturing difficulties and the likelihood of electrical shorts that may result from the presence of disjointed electrodes, a helical design was proposed where only two continuous electrodes were required.[254,255] The actuator was capable of a −5% compressive strain at a field of only 14 $MV \cdot m^{-1}$ using a softened silicone. A third configuration has also been proposed wherein a single long strip of DE film with electrodes on either side is simply folded in such a way as to keep the opposing electrodes isolated.[256–258] This configuration is perhaps the easiest to fabricate and yielded compressive strains and stresses up to 15% and ≈6 kPa respectively, but may result in non-uniform displacements. The three stacked actuator configurations are shown in Figure 21.

Another method to reduce manufacturing difficulties was developed by Schlaak et al.[259,260] They implemented a process wherein the components of a thermally cured silicone elastomer were spin-coated and thermally cured and the electrodes were spray-coated using a contact mask.

Recent efforts by Arora et al.[261] have led to the development of DE-based fiber actuators. These actuators are essentially miniaturized tube actuators. In their work, prestrain was applied by both uniaxial elongation as well as inflation. These actuators may be of interest for artificial muscle applications since the mimic the fibular nature of natural muscle; however, unlike natural muscle their method of actuation is through elongation and the maximum strains reported were limited to 7% in the axial direction. Cameron et al.[262] have performed similar work on coextruded tube DE actuators. Their co-extrusion process presents a fast, easy, scalable method to produce small diameter tubes, or hollow fibers, for use as DE actuators that

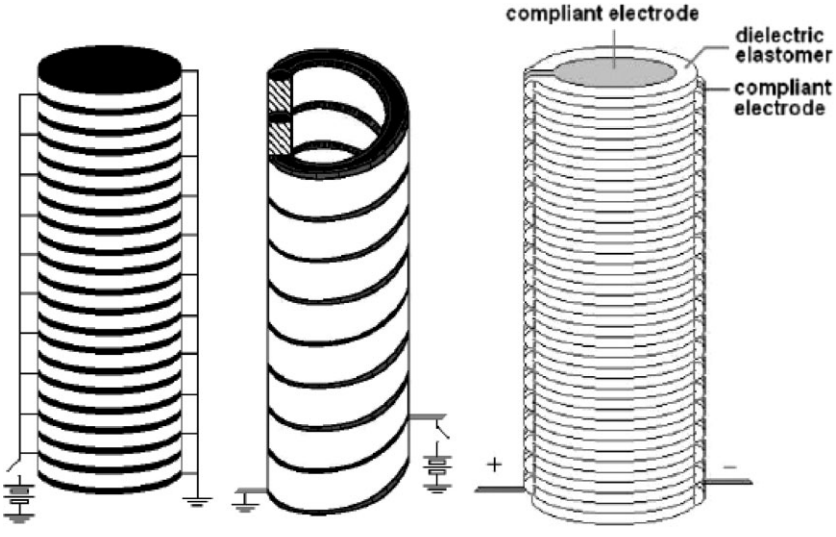

Figure 21. Stacked linear contractile actuator configurations. From left to right: Stacked device wherein alternating layers of elastomer and electrode are stacked together; helical device where two complementary helical elastomer strips and electrodes are interlocked; folded device where a single strip of elastomer with electrodes on the top and bottom is folded upon itself.[257]

would make these actuators very amenable to mass manufacturing. Strains, thus far, are limited to ≈2%.

The use of IPN films, describe in the DE Materials Section, have enabled higher energy density actuators. VHB-based IPN films seem particularly suited to the stacked actuator configuration as they do not require pre-straining. Kovacs and During[263] have recently reported on the fabrication of such an actuator. They constructed two prototypes, one consisting of 280 layers with an active diameter of 16 mm, a total diameter of 18 mm and a height of 18.3 mm; the second consisted of 330 layers, an active diameter of 16 mm, a total diameter of 20 mm and a height of 21.2 mm. The actuators achieved 46 and 35% contractile strain respectively with both ends free, and 30 and 20%, respectively, with their ends fixed to rigid supports. The reduced strain performance for devices with fixed ends was attributed to the physical constrains imposed by the rigid end pieces. The results were obtained at voltages just above 4 kV. Maximum forces achieved were in excess of 30 N. IPN films have also been incorporated in core free rolled actuators.[264] Since the film is free standing no spring core is needed to maintain prestrain in the film. As a result the shelf and actuation lifetime as well as the specific volume energy density of the device have been improved.

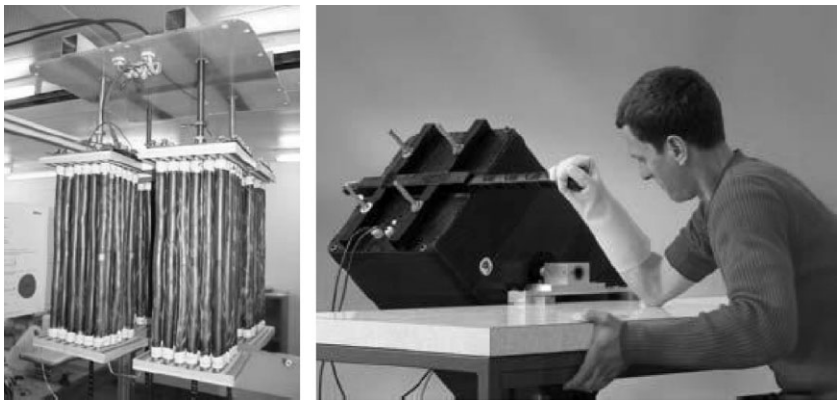

Figure 22. Arm wrestling robot using DE spring roll actuators. Left: actuator assemblies used in the device. Right: demonstration of the arm wrestling robot.[266]

DE Applications

DE Actuator Applications

When placed in an antagonistic arrangement, linear DE actuators have demonstrated the ability to mimic the motion of natural muscle. We are still some way off reliable reproduction of natural muscle's performance, however these preliminary results show a great deal of promise. When coupled with new advances in artificial skin and other related technologies that may reduce the performance requirements for artificial muscles, advances in DE actuators may allow for commercial applications sooner than would otherwise be anticipated.[265]

Perhaps the best example of both the promise that DE actuators and other EAP technologies show, and hurdles they must overcome, was the 2005 EAP arm wrestling competition put on by Bar-Cohen. Kovacs et al.[266] reported on the construction of one such robot as seen in Figure 22.

Other artificial muscle applications have been demonstrated as well. Carpi et al.[257,267,268] used helical contractile linear actuators and buckling actuators to actuate eyeballs for use in an android face. Another eyeball actuator has been developed by Liu et al.[240] based on their inflated actuator design; their actuator is capable of generating eyeball rotations from −50° to 50°. Kornbluh et al.[4] have also reported on a mouth driven by a DE actuator. Biddis and Chau[269] have provided a good review on the challenges and opportunities of DE actuators for upper limb prosthetics.

DE actuators have been used in a number of biomimitic robots ranging from simple hopping robots[270] and inchworm robots[4,271–274] to more complex walking robots, flapping-wing robots, and serpentine or octopus arm-inspired actuators.[4,237–239,274,275] Two particularly interesting walking robots developed by SRI, dubbed Flex II and MERbot, can be seen in Figure 23. Utilizing spring roll actuators, Flex 2 was capable of a respectable 3.5 $cm \cdot s^{-1}$.[274] MERbot used multiple-degree-of-freedom spring rolls to achieve speeds in excess of 13 $cm \cdot s^{-1}$.[251]

Potential applications of DE actuators are by no means limited to artificial muscles. A plethora of other DE applications have been proposed and demonstrated that can potentially be used in humanoid devices. These include loudspeakers,[276–278] variable diffraction gratings,[277] tunable transmission gratings,[279] and microoptical zoom lenses[280] among others. These applications may find use in biomimetics as a method to bestow polymer robots with the abilities to speak and focus their vision.

Outside of biomimetics, DEs may still be of use in other human-related applications including refreshable Braille devices,[259,281–283] hand-rehabilitation splints,[284] MRI-compatible machines,[246,285–287] microfluidic devices,[288–289] force-feedback,[249] and wearable tactile interfaces.[283,290] Other potential applications include actuators for lighter-than-air vehicles,[291,292] tunable phononic crystals,[293–295] and variable phase retarders.[296] Beck et al.[297] have also developed a sub-100 nm resolution total internal reflection fluorescence microscope using a tunable transmission grating and transparent phase shifters actuated by electro-active polymers.

Macromol. Rapid Commun. **2010**, *31*, 10–36

DOI: 10.1002/marc.200900425

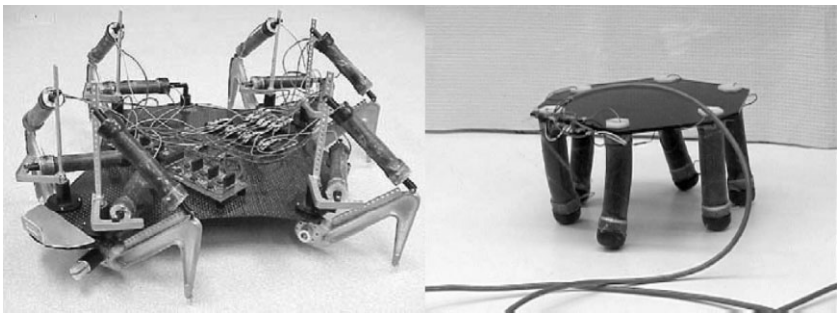

Figure 23. FLEX II and MERbot walking robots. FLEX II uses two DE spring roll actuators per leg while MERbot uses multidegree-of-freedom spring roll actuators.[251,274]

load. Ihlemfeld and Qu[306] have recently reported that an EAP actuator model with full electrical–mechanical dynamics can be used as a generator model with the generator input force equivalent to the actuator disturbance force. This is good news for the development of DE generators as the modeling work performed for actuator applications can be easily leveraged.

By monitoring the capacitance of the DE films, it is also possible to determine the level of strain in the elastomer.[307] In this manner, a DE device can also act as a strain or deflection sensor. Methods have also been developed that allow for transient strain analysis during actuation, allowing for the creation of "self-sensing" DE actuators with integrated extension sensors.[308–311] Chuc et al.[312] have also developed a "self-sensing" DE actuator capable of measuring the force exerted upon it. This "self-sensing" ability while undergoing actuation should make the development of controls systems easier and should allow for more compact device assemblies.

In certain configurations DEs may also be operated as spring elements with variable stiffness and damping characteristics.[4] If an actuator is held at a certain displacement, changing the applied electric field will vary the Maxwell stress across the device and thus the mechanical impedance.

The benefit of being able to sense deflections, generate energy, and modulate stiffness may have substantial impacts on the use of DEs as artificial muscles in robotic and prosthetic applications. The DE elements could act as artificial analogs of natural muscle, sensory systems, and digestive systems. A robot consisting of DE elements should therefore someday be capable of controlled motion without the need for additional sensors, and self-sustainability without requiring and external source of electricity.

Extending Applications of DEs

Since DEs behave essentially as variable capacitors, they may also be used as sensors and even as generators. Pelrine et al.[298] introduced the concept of DE generators in 2001. Several generator configurations have since been conceived.[4,277,298–303] Conceptually, DE devices can convert mechanical deformations into electrical energy based on the difference in capacitance between the device in the stretched and contracted states. If a bias voltage is applied across the electrodes in the stretched state with capacitance C_s, a certain amount of charge, Q, will be stored on the film at a potential V_b. If the film is then allowed to contract, the capacitance will decrease to a value C_c since the electrodes reduce in area and increase in separation. If the leakage current is negligible and no charge is allowed to flow off the DE device, then the amount of charge, Q, will remain unchanged but the potential of the charge will increase to $V_b + V_g$, where V_g is the electrical potential energy generated from the release of stored elastic energy in the elastomer. The generated energy, e_{gen}, can be estimated by taking the difference between the stored energy on the DE between the contracted and stretched states, e_c and e_s respectively

$$e_{gen} = e_c - e_s = \frac{1}{2}\left(C_c V_c^2 - C_s V_s^2\right) = \frac{1}{2} C_c \left(V_g^2 - V_b V_g\right) \quad (11)$$

The generated energy for a particular material can be maximized by operating the DE at a high bias field and stretching the film to large strains. The maximal energy that can be converted, however, is limited by a number of phenomena that impact both the generator and actuator modes of operation. These include electrical breakdown, EM instability (pull-in), loss of tension, and rupture by stretch.[304]

Jean-Mistral et al.[305] have developed a more complete model of the generator mode, incorporating viscous and hyperelastic effects. Their treatment takes into account viscous and electrical losses to produce more realistic estimates of the generated energy available to an external

Concluding Remarks

EAPs represent an important category of responsive materials for the transduction between electrical and mechanical energies. There are a diverse range of EAPs with distinctive actuation mechanisms and passive structural properties. Many EAPs exhibit modest to large actuation strain, specific energy density, modest to high actuation stress, on the same order of magnitude of performance as natural muscle. DEs appear to best reproduce the multifunctionality of muscles with unprecedented large actuation strain, high stress, specific energy density, and mechanical compliance. The high-performing DEs so far are largely commercial elastomers produced for

unrelated applications. Prestrain, IPN, or plasticizing additives further extend the breadth of the performance scope. There should be plenty of room for further improvement in the polymer materials development for high actuation speed, specific power density, and energy efficiency. The requirement for highly compliant electrodes is also essential, particularly with regard to patterning, fabrication complexity, and actuation stability. The available large strains have enabled a number of novel device configurations. This is an area that more exciting developments are expected as more engineers start to explore DE actuators. Commercial product developments are being pursued, though manufacturing yield and operational stability remain problematic. There are many more developers waiting for the driving voltage to come down, from kilovolts to the low hundreds of volts range. This could be achieved by either reducing the thickness of the extremely soft DE films to a few microns, which is a paramount manufacturing challenge, or by increasing the dielectric constant by two orders of magnitude, a goal that is being researched. In our opinion, the kV driving voltage is manageable as long as the overall power and stored energy are kept low. With proper insulation, DE actuators should be applicable to replace or augment muscle functions in biomimetic robots, prosthetic and implanted devices, and various controls.

Acknowledgements: We would like to thank all colleagues who have contributed to the development of electroactive polymers and whose works are cited here. Our special thanks go to Mr. *Wei Yuan*, Mr. *Soon Mok Ha*, Mr. *Zhibin Yu*, Ms. *Han Zhang*, and Ms. *Tuling Lam* of our laboratory, Dr. *Liangbin Hu* of UCLA Department of Physics, Dr. *Ron Pelrine*, Mr. *Roy Kornbluh*, and Mr. *Marcus Rosenthal* of SRI International for their works on dielectric elastomers. We would also like to acknowledge Dr. *Yoseph Bar-Cohen* of the Jet Propulsion Laboratory and Prof. *John Madden* of the University of British Columbia for creating and updating two of the most resourceful websites on EAPs, available online at http://eap.jpl.nasa.gov/ and http://actuatorweb.org/.

Received: June 16, 2009; Revised: August 19, 2009; Published online: October 27, 2009; DOI: 10.1002/marc.200900425

Keywords: artificial muscle; compliant electrode; dielectric elastomer; electroactive polymer; interpenetrating polymer networks

[1] "*Electroactive, Polymer (EAP) Actuators as Artificial Muscle*", Y. Bar-Cohen, Ed., 2nd edition, SPIE Press, Bellingham, WA 2004.
[2] J. D. Madden, N. A. Vandesteeg, P. A. Anquetil, P. G. Madden, A. Takshi, R. Z. Pytel, S. R. Lafontaine, P. A. Wieringa, W. Hunter, *IEEE J. Oceanic Eng.* **2004**, *29*, 706.
[3] R. Pelrine, R. Kornbluh, J. Joseph, R. Heydt, Q. Pei, S. Chiba, *Mater. Sci. Eng. C* **2000**, *11*, 89.
[4] R. Kornbluh, R. Pelrine, Q. Pei, R. Heydt, S. Stanford, S. Oh, J. Eckerle, *Proc. SPIE* **2002**, *4698*, 254.
[5] J. Hollerbach, I. Hunter, J. Ballantyne, *The Robotics Review*, Vol. 2, O. Khatib, J. Craig, T. Lozano-Perez, Eds., MIT Press, Cambridge, MA 1992, p. 299.
[6] Honda Motor Company, http://world.honda.com/ASIMO/.
[7] T. Mirfakhrai, J. D. Madden, R. Baughman, *Mater. Today* **2007**, *10*, 30.
[8] M. H. Dickinson, C. T. Farley, R. J. Full, M. A. R. Koehl, R. Kram, S. Lehman, *Science* **2000**, *288*, 100.
[9] I. Hunter, S. Lafontaine, *Tech. Dig. IEEE Solid State Sens. Actuators Workshop* 1992, p. 178.
[10] Y. Bar-Cohen, *Proc. SPIE* **2002**, *4695*, 1.
[11] Y. Bar-Cohen, *Proc. SPIE* **2004**, *5385*, 10.
[12] W. C. Roentgen, "*About the Changes in Shape and Volume of Dielectrics Caused by Electricity*", ser. Annual Physics and Chemistry Series, Vol. 11, sec III, G. Wiedemann, Eds., J. A. Barth Leipzig, Germany 1880, p. 771 German.
[13] S. Ashley, *Sci. Am.* **2003** (October issue) 52.
[14] R. Baughman, *Science* **2005**, *308*, 63.
[15] K. Meijer, M. Rosenthal, R. J. Full, *Proc. SPIE* **2001**, *4329*, 7.
[16] T. F. Otero, J. L. Cascales, A. J. Fernandez-Romero, *Proc. SPIE* **2007**, *6524*, 65240L.
[17] D. Trivedi, C. D. Rahn, W. M. Kier, I. D. Walker, *Appl. Bionics Biomech.* **2008**, *5*, 99.
[18] Z. Cheng, Q. Zhang, *MRS Bull.* **2008**, *33*, 183.
[19] A. M. Vinogradov, *Proc. SPIE* **2008**, *6927*, 69270M.
[20] J. L. Pons, "*Emerging Actuator Technologies: A Micromechatronic Approach*", Wiley, NJ 2005.
[21] J. E. Huber, N. A. Fleck, M. F. Ashby, *Proc. R. Soc. Lond. Ser. A* **1997**, *453*, 2185.
[22] S. G. Wax, R. R. Sands, *Proc. SPIE* **1999**, *3669*, 2.
[23] J. D. Madden, *Science* **2007**, *318*, 1094.
[24] R. Shankar, T. K. Ghosh, R. Spontak, *Soft Matter.* **2007**, *3*, 1116.
[25] A. O'Halloran, F. O'Malley, P. McHugh, *J. Appl. Phys.* **2008**, *104*, 071101.
[26] "*Electroactive Polymers for Robotic Applications: Artificial Muscles and Sensors*", K. J. Kim, S. Tadokoro, Eds., Springer, London, UK 2007.
[27] M. Shahinpoor, K. J. Kim, M. Mojarrad, "*Artificial Muscles: Applications of Advanced Polymeric Nanocomposites*", CRC Press Taylor & Francis Group, Boca Raton, FL 2007.
[28] "*Biomedical Applications of Electroactive Polymer Actuators*", F. Carpi, E. Smela, Eds., John Wiley & Sons Ltd., Chichester, West Sussex, UK 2009.
[29] M. Shahinpoor, K. J. Kim, *Smart Mater. Struct.* **2001**, *10*, 819.
[30] K. J. Kim, M. Shahinpoor, *Polymer* **2002**, *43*, 797.
[31] M. Shahinpoor, *Math. Mech. Solids* **2003**, *8*, 281.
[32] X.-L. Wang, I.-K. Oh, J. Lu, J. Ju, S. Lee, *Mater. Lett.* **2007**, *61*, 5117.
[33] S. Nemat-Nasser, *J. Appl. Phys.* **2002**, *92*, 2899.
[34] M. Shahinpoor, K. J. Kim, *Smart Mater. Struct.* **2005**, *14*, 197.
[35] K. Kaneto, M. Kaneko, Y. Min, A. G. MacDiarmid, *Synth. Met.* **1995**, *71*, 2211.
[36] B. J. Akle, M. D. Bennett, D. J. Leo, *Sens. Actuators A* **2006**, *126*, 173.
[37] S. Nemat-Nasser, Y. X. Wu, *J. Appl. Phys.* **2003**, *93*, 5255.
[38] K. J. Kim, M. Shahinpoor, *Smart Mater. Struct.* **2003**, *12*, 65.
[39] Eamax Co., Japan, http://www.eamex.co.jp/.
[40] W. Kuhn, B. Hargitay, A. Katchalsky, H. Eisenberg, *Nature (London)* **1955**, *165*, 514.
[41] A. Katchalsky, M. Zwick, *J. Polym. Sci.* **1955**, *16*, 221.
[42] A. Fragala, J. Enos, A. Laconti, J. Boyack, *Electrochim. Acta* **1972**, *17*, 1507.
[43] Y. Osada, *Adv. Polym. Sci.* **1987**, *82*, 1.

DOI: 10.1002/marc.200900425

[44] T. Tanaka, *Polymer* **1979**, *20*, 1404.
[45] Y. Osada, M. Hasebe, *Chem. Lett.* **1985**, *9*, 1285.
[46] T. Shiga, *Adv. Polym. Sci.* **1997**, *134*, 131.
[47] P. Calvert, Z. Liu, *Acta Metall. Mater.* **1998**, *46*, 2565.
[48] Z. S. Liu, P. Calvert, *Adv. Mater.* **2000**, *12*, 288.
[49] B. Tondu, R. Emirkhanian, S. Mathé, A. Ricard, *Sens. Actuators A* **2009**, *150*, 124.
[50] S. Iijima, *Nature* **1991**, *354*, 56.
[51] R. H. Baughman, A. A. Zakhidov, W. A. de Heer, *Science* **2002**, *297*, 787.
[52] R. H. Baughman, C. Chanxing, A. A. Zakhidov, Z. Iqbal, J. N. Barisci, G. M. Spinks, G. G. Wallace, A. Mazzoldi, D. De Rossi, A. G. Rinzler, O. Jaschinski, S. Roth, M. Kertesz, *Science* **1999**, *284*, 1340.
[53] J. D. W. Madden, J. N. Barisci, P. A. Anquetil, G. M. Spinks, G. G. Wallace, R. H. Baughman, I. W. Hunter, *Adv. Mater.* **2006**, *18*, 870.
[54] T. Mirfakhrai, J. D. W. Madden, R. H. Baughman, *Smart Mater. Struct.* **2006**, *16*, S243.
[55] M. K. Shin, S. I. Kim, S. J. Kim, S.-K. Kim, H. Lee, G. M. Spinks, *Appl. Phys. Lett.* **2006**, *89* 231929.
[56] M. Hughes, G. M. Spinks, *Adv. Mater.* **2005**, *17*, 443.
[57] Y. L. Li, I. A. Kinloch, A. H. Windle, *Science* **2004**, *304*, 276.
[58] R. H. Baughman, *Nat. Nanotechnol.* **2006**, *1*, 94.
[59] A. E. Aliev, J. Oh, M. E. Kozlov, A. A. Kuznetsov, S. Fang, A. F. Fonseca, R. Ovalle, M. D. Lima, M. H. Haque, Y. N. Gartstein, M. Zhang, A. A. Zakhidov, R. H. Baughman, *Science* **2009**, *323*, 1575.
[60] R. H. Baughman, L. W. Shacklette, R. L. Elsebaumer, E. J. Plichta, C. Becht, "*Conjugated Polymeric Materials: Opportunities in Electronics, Optoelectronics, and Molecular Electronics*", J. L. Brédas, R. R. Chance, Eds., Kluwer, Dordrecht 1990, p. 559.
[61] R. H. Baughman, L. W. Shacklette, R. L. Elsebaumer, E. J. Plichta, C. Becht, "*Topics in Molecular Organization and Engineering: Molecular Electronics*", Vol. 7, P. I. Lazarev, Ed., Kluwer, Dordrecht 1991, p. 267.
[62] R. H. Baugman, *Makromol. Chem. Macromol. Symp.* **1991**, *51*, 193.
[63] R. H. Baughman, *Synth. Met.* **1996**, *78*, 339.
[64] Q. Pei, O. Inganäs, *Adv. Mater.* **1992**, *4*, 277.
[65] E. Smela, O. Inganäs, I. Lundström, *Science* **1995**, *268*, 1735.
[66] T. F. Otero, E. Angulo, J. Rodriguez, C. Santamaria, *J. Electroanal. Chem.* **1992**, *341*, 369.
[67] T. E. Herod, J. B. Schlenoff, *Chem. Mater.* **1993**, *5*, 951.
[68] R. S. Pytel, E. Thomas, I. Hunter, *Chem. Mater.* **2006**, *18*, 861.
[69] Q. Pei, O. Inganäs, *J. Phys. Chem.* **1992**, *96*, 10507.
[70] Q. Pei, O. Inganäs, *Solid State Ionics* **1993**, *60*, 161.
[71] Q. Pei, O. Inganäs, *J. Phys. Chem.* **1993**, *97*, 6034.
[72] Q. Pei, O. Inganas, I. Lundstrom, *Smart Mater. Struct.* **1993**, *2*, 1.
[73] A. Mazzoldi, A. Della Santa, D. De Rossi, "*Conducting polymer actuators: Properties and modeling, In: Polymer Sensors and Actuators*", Y. Osada, D. E. De Rossi, Eds., Springer Verlag, Heidelberg 1999, p. 207.
[74] M. Cole, J. D. Madden, *Mater. Res. Soc. Symp. Proc.* **2005**, *889*, W04.
[75] E. Smela, N. Gadegaard, *Adv. Mater.* **1999**, *11*, 953.
[76] S. Hara, T. Zama, W. Takashima, K. Kaneto, *Polym. J.* **2004**, *36*, 151.
[77] S. Hara, T. Zama, W. Takashima, K. Kaneto, *Synth. Met.* **2006**, *156*, 351.
[78] G. M. Spinks, V. Mottaghitalab, M. Bahrami-Samani, P. G. Whitten, G. G. Wallace, *Adv. Mater.* **2006**, *18*, 637.
[79] K. Kaneto, M. Kaneko, Y. Min, A. G. MacDiarmid, *Synth. Met.* **1995**, *71*, 2211.
[80] T. W. Lewis, L. A. P. Kane-Maguire, A. S. Hutchinson, G. M. Spinks, G. G. Wallace, *Synth. Met.* **1999**, *102*, 1317.
[81] G. M. Spinks, G. G. Wallace, J. Ding, D. Zhou, B. Xi, T. R. Scott, V.-T. Truong, *Proc. SPIE* **2003**, *5051*, 372.
[82] P. F. Pettersson, E. W. H. Jager, O. Inganas, "*1st Int. IEEE-EMBS Special Topic Conf. Microtechnol. Med. Biol.* " A. Dittmar, D. Beebe, Eds., IEEE-EMBS, Lyon, France 2000, 334.
[83] A. DellaSanta, et al. *J. Intell. Mater. Sys. Struct.* **1996**, *7*, 292.
[84] Y. Takase, J. W. Lee, J. I. Scheinbeim, B. A. Newman, *Macromolecules* **1991**, *24*, 6644.
[85] J. Su, Z. Y. Ma, J. I. Scheinbeim, B. A. Newman, *J. Polym. Sci. B* **1995**, *33*, 85.
[86] Q. Gao, J. I. Scheinbeim, B. A. Newman, *Macromolecules* **2000**, *33*, 7564.
[87] A. J. Lovinger, G. T. Davis, T. Furukawa, M. G. Broadhurst, *Macromolecules* **1982**, *15*, 323.
[88] A. J. Lovinger, "*Developments in Crystalline Polymers-1*", D. C. Bassett, Ed., Applied Science Publishers, London 1982, p. 195.
[89] A. J. Lovinger, T. Furukawa, *Ferroelectrics* **1983**, *50*, 227.
[90] Y. Xu, "*Ferroelectric Materials and Their Applications*", North-Holland, Netherlands 1991.
[91] C. Huang, R. Klein, F. Xia, H. Li, Q. M. Zhang, F. Bauer, Z.-Y. Cheng, *IEEE Trans. Dielectr. Electr. Insul.* **2004**, *11*, 299.
[92] K. K. Tashiro, M. Takano, Y. Kobayashi, A. Chatani, H. Tadokoro, *Ferroelectrics* **1984**, *57*, 297.
[93] Q. M. Zhang, J. Zhao, T. Shrout, N. Kim, L. E. Cross, A. Amin, B. M. Kulwicki, *J. Appl. Phys.* **1995**, *77*, 2549.
[94] M. Eguchi, *Philos. Mag.* **1925**, *49*, 178.
[95] G. M. Sessler, Ed., "*Electrets*", 3rd edition, *Vol. 1*, Laplacian Press, Morgan Hill, California, USA 1998.
[96] S. Bauer, *IEEE Trans. Dielectr. Electr. Insul.* **2006**, *13*, 953.
[97] S. Bauer, R. Gerhard-Multhaupt, G. Sessler, *Phys. Today* **2004**, *57*, 37.
[98] D. Lovera, H. Ruckdäschel, A. Göldel, N. Behrendt, T. Frese, J. K. W. Sandler, B. Altstädt, R. Giesa, H.-W. Schmidt, *Eur. Polym. J.* **2007**, *43*, 1195.
[99] Z.-Y. Cheng, R. S. Katiyar, X. Yao, A. S. Bhalla, *Phys. Rev. B* **1998**, *57*, 8166.
[100] Z.-Y. Cheng, Q. M. Zhang, F. B. Bateman, *J. Appl. Phys.* **2002**, *92*, 6749.
[101] Q. M. Zhang, V. Bharti, X. Zhao, *Science* **1998**, *280*, 2101.
[102] C. Huang, R. Klein, F. Xia, H. F. Li, Q. M. Zhang, F. Bauer, Z.-Y. Cheng, *IEEE Trans. Dielectr. Electr. Insul.* **2004**, *11*, 299.
[103] Z.-Y. Cheng, T.-B. Xu, V. Bharti, S. Wang, Q. M. Zhang, *Appl. Phys. Lett.* **1999**, *74*, **1901**.
[104] S. Guo, X.-Z. Zhao, Q. Zhuo, H. L. W. Chan, C. L. Choy, *Appl. Phys. Lett.* **2004**, *84*, 3349.
[105] F. Xia, Z.-Y. Cheng, H. Xu, H. Li, Q. M. Zhang, G. Kavarnos, R. Ting, G. Abdul-Sedat, K. D. Belfield, *Adv. Mater.* **2002**, *14*, 1574.
[106] H. Xu, Z.-Y. Cheng, D. Olson, T. Mai, Q. M. Zhang, G. Kavarnos, *Appl. Phys. Lett.* **2001**, *78*, 2360.
[107] J. T. Garrett, C. M. Roland, A. Petchsuk, T. C. Chung, *Appl. Phys. Lett.* **2003**, *83*, 1190.
[108] A. C. Jayasuriya, A. Schirokauer, J. I. Scheinbeim, *J. Polym. Sci., Part B: Polym. Phys.* **2001**, *39*, 2793.
[109] M. Wegener, J. Hesse, K. Richter, R. Gerhard-Multhaupt, *J. Appl. Phys.* **2002**, *92*, 7442.
[110] B. Neese, Y. Wang, B. J. Chu, K. L. Ren, S. Liu, Q. M. Zhang, C. Huang, J. West, *Appl. Phys. Lett.* **2007**, *90*, 242917.

[111] H.-M. Bao, C.-L. Jia, C.-C. Wang, Q.-D. Shen, C.-Z. Yang, Q. M. Zhang, *Appl. Phys. Lett.* **2008**, *92*, 042903.
[112] F. Xia, H. Li, C. Huang, M. Y. M. Huang, H. Xu, F. Bauer, Z.-Y. Cheng, Q. M. Zhang, *Proc. SPIE* **2003**, *5051*, 133.
[113] J. Su, K. Hales, T.-B. Xu, *Proc. SPIE* **2003**, *5051*, 191.
[114] J. Su, J. S. Harrison, T. L. S. Clair, Y. Bar-Cohen, S. Leary, *Mater. Res. Soc. Symp. Proc.* **1999**, *600*, 131.
[115] M. Warner, M. Terentjev, "*Liquid Crystal Elastomers*", Oxford Science Publications, Oxford, UK 2003.
[116] P. G. de Gennes, T. C. Chung, A. Petchsux, *Seances Acad. Sci. Ser. B* **1975**, *281*, 101.
[117] P.-G. de Gennes, *CR Acad. Sci. Paris Ser. IIb* **1997**, *324*, 343.
[118] D. L. Thomsen, P. Keller, J. Naciri, R. Pink, H. Jeon, D. Shenoy, B. R. Ratna, *Macromolecules* **2001**, *34*, 5868.
[119] H. Wermter, H. Finkelmann, *e-Polymers* **2001**, *13*, 1, http://www.e-polymers.org.
[120] M.-H. Li, P. Keller, *Phil. Trans. R. Soc. A* **2006**, *364*, 2763.
[121] W. Lehmann, H. Skupin, C. Tolksdorf, E. Gebhard, R. Zentel, P. Kruger, M. Losche, F. Kremer, *Nature* **2001**, *410*, 447.
[122] P.-G. de Gennes, "Polymer Liquid Crystals", in: *Mechanical Properties of Nematic Polymers*, A. Cifferi, W. R. Krigbaum, R. B. Meyer, Eds., Academic Press, New York, NY 1982, p. 115.
[123] J.-F. D'Allest, P. Maissa, A. Ten Bosch, P. Sixou, A. Blumstein, R. B. Blumstein, J. Teixeira, L. Noirez, *Phys. Rev. Lett.* **1988**, *61*, 2562.
[124] M.-H. Li, A. Brûlet, P. Davidson, P. Keller, J.-P. Cotton, *Phys. Rev. Lett.* **1993**, *70*, 2297.
[125] M.-H. Li, A. Brûlet, J.-P. Cotton, P. Davidson, C. Strazielle, P. Keller, *J. Phys. II France* **1994**, *4*, 1843.
[126] W. Lehmann, L. Hartmann, F. Kremer, P. Stein, H. Finkelmann, H. Kruth, S. Diele, *J. Appl. Phys.* **1999**, *86*, 1647.
[127] N. Leister, W. Lehmann, U. Weber, D. Geschke, F. Kremer, P. Stein, H. Finkelmann, *Liq. Cryst.* **2000**, *27*, 289.
[128] S. S. Roy, W. Lehmann, E. Gebhard, C. Tolksdorf, R. Zentel, F. Kremer, *Mol. Cryst. Liq. Cryst.* **2002**, *375*, 253.
[129] D. K. Shenoy, D. L. Thomsen, A. Srinivasan, P. Keller, B. R. Ratna, *Sens. Actuators A* **2002**, *96*, 184.
[130] H. Skupin, F. Kremer, S. V. Shilov, P. Stein, H. Finkelmann, *Macromolecules* **1999**, *32*, 3746.
[131] C. H. Huang, Q. Zhang, A. Jakli, *Adv. Funct. Mater.* **2003**, *13*, 525.
[132] H. Finkelmann, M. Shahinpoor, *Proc. SPIE* **2002**, *4695*, 459.
[133] H. Finkelmann, H. Wermter, *ACS Abstr.* **2000**, *219*, 189.
[134] S. V. Ahir, A. R. Tajbakhsh, E. M. Terentjev, *Adv. Funct. Mater.* **2006**, *16*, 556.
[135] J. Naciri, A. Srinivasan, H. Joen, N. Nikolov, P. Keller, B. R. Ratna, *Macromolecules* **2003**, *36*, 8499.
[136] M. Chambers, H. Finkelmann, M. Remskar, A. Sánchez-Ferrer, B. Zalar, S. Zumer, *J. Mater. Chem.* **2009**, *19*, 1524.
[137] C. M. Spillmann, B. R. Ratna, J. Naciri, *Appl. Phys. Lett.* **2007**, *90* 021911.
[138] D. M. Walba, H. Yang, R. K. Shoemaker, P. Keller, R. Shao, D. A. Coleman, C. D. Jones, M. Nakata, N. A. Clark, *Chem. Mater.* **2006**, *18*, 4576.
[139] R. E. Pelrine, R. D. Kornbluh, J. P. Joseph, *Sens. Actuators A* **1998**, *64*, 77.
[140] I. Krakovsky, T. Romjin, A. Posthuma de Boer, *J. Appl. Phys.* **1999**, *85*, 628.
[141] R. Pelrine, R. Kornbluh, Q. Pei, J. Joseph, *Science* **2000**, *287*, 836.
[142] R. Díaz-Calleja, M. J. Sanchis, E. Riande, *J. Electrostat.* **2009**, *67*, 158.
[143] N. Goulbourne, E. Mockensturm, M. Frecker, *J. Appl. Mech.* **2005**, *72*, 899.
[144] M. Wissler, E. Mazza, *Sens. Actuators A* **2005**, *120*, 184.
[145] G. Kofod, "Dielectric Elastomer Actuators" *Ph.D. Thesis* The Technical University of Denmark, September 2001.
[146] M. Wissler, E. Mazza, *Smart Mater. Struct.* **2005**, *14*, 1396.
[147] P. Sommer-Larsen, G. Kofod, M. H. Shridhar, M. Benslimane, P. Gravesen, *Proc. SPIE* **2002**, *4695*, 158.
[148] E. Yang, M. Frecker, E. Mockensturm, *Proc. SPIE* **2005**, *5759*, 82.
[149] J.-S. Plante, S. Dubowsky, *Sens. Actuators A* **2007**, *137*, 96.
[150] M. Wissler, E. Mazza, *Sens. Actuators A* **2007**, *138*, 384.
[151] H. W. Hwang, C.-J. Kim, S. J. Kim, H. Yang, N. C. Park, Y.-P. Park, *Proc. SPIE* **2008**, *6927*, 692726.
[152] X. Zhao, Z. Suo, *J. Appl. Phys.* **2008**, *104*, 123530.
[153] J. W. Fox, N. C. Goulbourne, *J. Mech. Phys. Solids* **2008**, *56*, 2669.
[154] J. W. Fox, N. C. Goulbourne, *Proc. SPIE* **2008**, *6927*, 69271P.
[155] R. Kornbluh, R. Pelrine, J. Joseph, R. Heydt, Q. Pei, S. Chiba, *Proc. SPIE* **1999**, *3669*, 149.
[156] J. Zhou, W. Hong, X. Zhao, Z. Zhang, Z. Suo, *Int. J. Solids Struct.* **2008**, *45*, 3739.
[157] M. Moscardo, X. Zhao, Z. Suo, Y. Lapusta, *J. Appl. Phys.* **2008**, *104*, 093503.
[158] J. S. Plante, S. Dubowsky, *Int. J. Solids Struct.* **2006**, *43*, 7727.
[159] X. Zhao, W. Hong, Z. Suo, *Phys. Rev. B* **2007**, *76*, 134113.
[160] R. Díaz-Calleja, E. Riande, M. J. Sanchis, *Appl. Phys. Lett.* **2008**, *93* 101902.
[161] J. Leng, L. Liu, Y. Liu, K. Yu, S. Sun, *Appl. Phys. Lett.* **2009**, *94* 211901.
[162] R. Pelrine, R. Kornbluh, J. Joseph, S. Chiba, *IEEE Tenth Annual International Workshop on MEMS* 1997, p. 238.
[163] R. Pelrine, R. Kornbluh, G. Kofod, *Adv. Mater.* **2000**, *12*, 1223.
[164] R. Kornbluh, R. Pelrine, Q. Pei, S. Oh, J. Joseph, *Proc. SPIE* **2000**, *3987*, 51.
[165] F. Carpi, A. Mazzoldi, D. De Rossi, *Proc. SPIE* **2003**, *5051*, 419.
[166] G. Kofod, P. Sommer-Larsen, R. Kornbluh, R. Pelrine, *J. Intell. Mater. Syst. Struct.* **2003**, *14*, 787.
[167] J.-S. Plante, S. Dubowsky, *Int. J. Solids Struct.* **2006**, *43*, 7727.
[168] G. Kofod, R. Kornbluh, R. Pelrine, P. Sommer-Larsen, *Proc. SPIE* **2001**, *4329*, 141.
[169] X. Zhao, Z. Suo, *Appl. Phys. Lett.* **2007**, *91* 061921.
[170] R. Palakodeti, M. R. Kessler, *Mater. Lett.* **2006**, *60*, 3437.
[171] H. R. Choi, K. Jung, N. H. Chuc, M. Jung, I. Koo, J. Koo, J. Lee, J. Lee, J. Nam, M. Cho, Y. Lee, *Proc. SPIE* **2005**, *5759*, 283.
[172] P. Lochmatter, G. Kovacs, M. Wissler, *Smart Mater. Struct.* **2007**, *16*, 477.
[173] A. Wissler, E. Mazza, *Sens. Actuators A* **2005**, *120*, 184.
[174] Q. Pei, R. Pelrine, S. Stanford, R. Kornbluh, M. Rosenthal, *Synth. Met.* **2003**, *135–136*, 129.
[175] N. C. Goulbourne, E. M. Mockensturm, M. I. Frecker, *Int. J. Solids Struct.* **2007**, *44*, 2609.
[176] N. Goulbourne, E. Mockensturm, M. Frecker, *J. Appl. Mech.* **2005**, *72*, 899.
[177] P. Lochmatter, G. Kovacs, *Sens. Actuators A* **2008**, *141*, 577.
[178] P. Lochmatter, G. Kovacs, M. Silvain, *Sens. Actuators A* **2007**, *135*, 748.
[179] E. M. Mockensturm, N. Goulbourne, *Int. J. Non-Linear Mech.* **2006**, *41*, 388.
[180] M. Wissler, E. Mazza, *Sens. Actuators A* **2007**, *134*, 494.
[181] M. Wissler, E. Mazza, *Sens. Actuators A* **2007**, *138*, 384.
[182] G. Kofod, *J. Phys. D: Appl. Phys.* **2008**, *41*, 215405.
[183] C. Huang, Q. M. Zhang, G. deBotton, K. Bhattacharya, *Appl. Phys. Lett.* **2004**, *84*, 4391.
[184] G. Gallone, F. Carpi, D. De Rossi, G. Levita, A. Marchetti, *Mater. Sci. Eng. C* **2007**, *27*, 110.

Macromolecular Journals
DOI: 10.1002/marc.200900425

[185] Z. Zhang, L. Liu, J. Fan, K. Yu, L. Shi, J. Leng, *Proc. SPIE* **2008**, *6926*, 692610.
[186] P. Lotz, M. Matysek, P. Lechner, M. Hamann, H. F. Schlaak, *Proc. SPIE* **2008**, *6927*, 692723.
[187] J. P. Szabo, J. A. Hiltz, C. G. Cameron, R. S. Underhill, J. Massey, B. White, J. Leidner, *Proc. SPIE* **2003**, *5051*, 180.
[188] F. Carpi, D. De Rossi, *IEEE Trans. Dielectr. Electr. Insul.* **2005**, *12*, 835.
[189] M. Razzaghi-Kashani, N. Gharavi, S. Javadi, *Smart Mater. Struct.* **2008**, *17*, 065035.
[190] X. Q. Zhang, M. Wissler, B. Jaehne, R. Broennimann, G. Kovacs, *Proc. SPIE* **2004**, *5385*, 78.
[191] W. Wichiansee, A. Sirivat, *Mater. Sci. Eng. C* **2009**, *29*, 78.
[192] F. Carpi, G. Gallone, F. Galantini, D. De Rossi, *Adv. Funct. Mater.* **2008**, *18*, 235.
[193] L. Z. Chen, C. H. Chen, C. H. Hu, S. S. Fan, *Appl. Phys. Lett.* **2008**, *92*, 263104.
[194] Q. Pei, R. Pelrine, M. Rosenthal, S. Stanford, H. Prahlad, R. Kornbluh, *Proc. SPIE* **2004**, *5385*, 41.
[195] G. Mathew, J. M. Rhee, C. Nah, D. J. Leo, C. Nah, *Polym. Eng. Sci.* **2006**, *46*, 1455.
[196] S. M. Ha, W. Yuan, Q. Pei, R. Pelrine, S. Stanford, *Adv. Mater.* **2006**, *18*, 887.
[197] S. M. Ha, W. Yuan, Q. Pei, R. Pelrine, S. Stanford, *Proc. SPIE* **2006**, *6168*, 616808.
[198] S. M. Ha, W. Yuan, Q. Pei, R. Pelrine, S. Stanford, *Smart Mater. Struct.* **2007**, *16*, S280.
[199] S. M. Ha, M. Wissler, R. Pelrine, S. Stanford, G. Kovacs, Q. Pei, *Proc. SPIE* **2007**, *6524*, 652408.
[200] S. M. HA, I. S. Park, M. Wissler, R. Pelrine, S. Stanford, K. J. Kim, G. Kovacs, Q. Pei, *Proc. SPIE* **2008**, *6927*, 69272C.
[201] R. Shankar, T. K. Ghosh, R. J. Spontak, *Adv. Mater.* **2007**, *19*, 2218.
[202] R. Shankar, T. K. Ghosh, R. J. Spontak, *Macromol. Rapid Commun.* **2007**, *28*, 1142.
[203] R. Shankar, T. K. Ghosh, R. J. Spontak, *Sens. Actuators A* **2009**, *151*, 46.
[204] Q. M. Zhang, J. Su, C. H. Kim, R. Ting, R. Capps, *J. Appl. Phys.* **1997**, *81*, 2770.
[205] C. G. Cameron, R. S. Underhill, M. Rawji, J. P. Szabo, *Proc. SPIE* **2004**, *5385*, 51.
[206] J.-D. Nam, S. D. Hwang, H. R. Choi, J. H. Lee, K. J. Kim, S. Heo, *Smart Mater. Struct.* **2005**, *14*, 87.
[207] B. Guiffard, L. Seveyrat, G. Sebald, D. Guyomar, *J. Phys. D: Appl. Phys.* **2006**, *39*, 3053.
[208] L. Petit, B. Guiffard, L. Seveyrat, D. Guyomar, *Sens. Actuators A* **2008**, *148*, 105.
[209] Q. M. Zhang, H. Li, M. Poh, F. Xia, Z.-Y. Cheng, H. Xu, C. Huang, *Nature* **2002**, *419*, 284.
[210] K. Jung, J. H. Lee, M. S. Cho, J. C. Koo, J. Nam, Y. K. Lee, H. R. Choi, *Proc. SPIE* **2006**, *6168*, 61680N.
[211] K. Jung, J. Lee, M. Cho, J. C. Koo, J. Nam, Y. Lee, H. R. Choi, *Smart Mater. Struct.* **2007**, *16*, S288.
[212] H. C. Nguyen, V. T. Doan, J. Park, J. C. Koo, Y. Lee, J. Nam, H. R. Choi, *Smart Mater. Struct.* **2009**, *18*, 015006.
[213] F. Carpi, P. Chiarelli, A. Mazzoldi, D. De Rossi, *Sens. Actuators A* **2003**, *107*, 85.
[214] M. Benslimane, P. Gravesen, *Proc. SPIE* **2002**, *4695*, 150.
[215] S. P. Lacour, S. Wagner, Z. Huang, Z. Suo, *Appl. Phys. Lett.* **2003**, *82*, 2404.
[216] J. H. Lalli, S. Hannah, M. Bortner, S. Subrahmanyan, J. Mecham, B. Davis, R. O. Claus, *Proc. SPIE* **2004**, *5385*, 290.
[217] A. B. Hill, R. O. Claus, J. H. Lalli, J. B. Mecham, B. A. Davis, R. M. Goff, S. Subrahmanyan, *Proc. SPIE* **2005**, *5759*, 246.
[218] R. O. Claus, R. M. Goff, M. Homer, A. B. Hill, J. H. Lalli, *Proc. SPIE* **2006**, *6168*, 61681O.
[219] R. Delille, M. Urdaneta, K. Hseih, E. Smela, *Proc. SPIE* **2006**, *6168*, 61681Q.
[220] S. Rosset, M. Niklaus, P. Dubois, H. R. Shea, *Sens. Actuators A* **2008**, *144*, 185.
[221] S. Rosset, M. Niklaus, V. Stojanov, A. Felber, P. Dubois, H. R. Shea, *Proc. SPIE* **2008**, *6927*, 69270W.
[222] S. Rosset, M. Niklaus, P. Dubois, H. R. Shea, *IEEE MEMS 2008* Tucson, AZ, USA, January 13–17 2008, p. 503.
[223] S. Rosset, M. Niklaus, P. Dubois, H. R. Shea, *Adv. Funct. Mater.* **2009**, *19*, 470.
[224] W. Yuan, T. Lam, J. Biggs, L. Hu, Z. Yu, S. M. Ha, D. Xi, M. K. Senesky, G. Grűner, Q. Pei, *Proc. SPIE* **2007**, *6524*, 65240N.
[225] T. Lam, H. Tran, W. Yuan, Z. Yu, S. M. Ha, R. Kaner, Q. Pei, *Proc. SPIE* **2008**, *6927*, 69270O.
[226] W. Yuan, L. Hu, S. Ha, T. Lam, G. Grűner, Q. Pei, *Proc. SPIE* **2008**, *6927*, 69270P.
[227] W. Yuan, L. Hu, Z. Yu, T. Lam, J. Biggs, S. M. Ha, D. Xi, B. Chen, M. K. Senesky, G. Grűner, Q. Pei, *Adv. Mater.* **2008**, *20*, 621.
[228] L. Hu, W. Yuan, P. Brochu, G. Gruner, Q. Pei, *Appl. Phys. Lett.* **2009**, *94*, 161108.
[229] W. Yuan, P. Brochu, H. Zhang, A. Jan, Q. Pei, *Proc. SPIE* **2009**, *7287*, 72870O.
[230] R. Kornbluh, R. Pelrine, J. Joseph, *Proceedings of the Third IASTED International Conference on Robotics and Manufacturing, Cancun*, Mexico, June 14–16, 1995 (ACTA Press, Calgary, Alberta, 1995), p. 1.
[231] R. Kornbluh, R. Pelrine, J. Eckerle, J. Joseph, *Proceedings of the 1998 IEEE International Conference on Robotics and Automation*, Leuven, Belgium, May 1998 (IEEE Press, Piscataway, NJ, 1998), p. 2147.
[232] F. Carpi, D. De Rossi, R. Kornbluh, R. Pelrine, P. Sommer-Larsen, Eds., *"Dielectric Elastomers as Electromechanical Transducers: Fundamentals, Materials, Devices, Models and Applications of an Emerging Electroactive Polymer Technology"* Elsevier Ltd., Oxford, UK 2008.
[233] H. Choi, S. Ryew, K. Jung, J. Jeon, H. Kim, J. Nam, A. Takanishi, R. Maeda, K. Kaneko, K. Tanie, *Proc. SPIE* **2002**, *4695*, 138.
[234] H. R. Choi, K. M. Jung, J. W. Kwak, S. W. Lee, H. M. Kim, J. W. Jeon, J. D. Nam, *Proc. SPIE* **2003**, *5051*, 262.
[235] M. Y. Jung, N. H. Chuc, J. W. Kim, I. M. Koo, K. M. Jung, Y. K. Lee, J. D. Nam, H. R. Choi, J. C. Koo, *Proc. SPIE* **2006**, *6168*, 616824.
[236] N. C. S. Goulbourne, *Proc. SPIE* **2006**, *6168*, 61680A.
[237] P. Lochmatter, G. Kovacs, *Proc. SPIE* **2007**, *6524*, 65241O.
[238] H. Wang, J. Zhu, *Proc. SPIE* **2008**, *7266*, 726607.
[239] *"Advances in Robot Kinematics: Analysis and Design"*, J. Lenarcic, P. Wenger, Eds., Springer Science+Business Media B.V, Berlin, Germany 2008, p. 291.
[240] Y. Liu, L. Shi, L. Liu, Z. Zhang, J. Leng, *Proc. SPIE* **2008**, *6927*, 69271A.
[241] H. Prahlad, R. Pelrine, R. Kornbluh, P. von Guggenberg, S. Chhokar, J. Eckerle, *Proc. SPIE* **2005**, *5759*, 102.
[242] F. Carpi, D. De Rossi, *Mater. Sci. Eng. C* **2004**, *24*, 555.
[243] G. Kofod, M. Paajanen, S. Bauer, *Proc. SPIE* **2006**, *6168*, 61682J.
[244] G. Kofod, W. Wirges, M. Paajanen, S. Bauer, *Appl. Phys. Lett.* **2007**, *90* 081916.
[245] B. O'Brien, E. Calius, S. Xie, I. Anderson, *Proc. SPIE* **2008**, *6927*, 69270T.
[246] J.-S. Plante, L. M. Devita, S. Dubowsky, *Proc. SPIE* **2007**, *6524*, 652406.

[247] N. Bonwit, J. Heim, M. Rosenthal, C. Duncheon, A. Beavers, *Proc. SPIE* **2006**, *6168*, 616805.
[248] Q. Pei, R. Pelrine, S. Stanford, R. Kornbluh, M. Rosenthal, *Synth. Met.* **2003**, *135–136*, 129.
[249] R. Zhang, P. Lochmatter, A. Kunz, G. Kovacs, *Proc. SPIE* **2006**, *6168*, 61681T.
[250] Q. Pei, M. Rosenthal, R. Pelrine, S. Stanford, R. Kornbluh, *Proc. SPIE* **2003**, *5051*, 281.
[251] Q. Pei, M. Rosenthal, S. Stanford, H. Prahlad, R. Pelrine, *Smart Mater. Struct.* **2004**, *13*, N86.
[252] Q. Pei, R. Pelrine, M. Rosenthal, S. Stanford, H. Prahlad, R. Kornbluh, *Proc. SPIE* **2004**, *5385*, 41.
[253] N. H. Chuc, J. Park, D. V. Thuy, H. S. Kim, J. Koo, Y. Lee, J. Nam, H. R. Choi, *Proc. SPIE* **2007**, *6524*, 65240J.
[254] F. Carpi, A. Migliore, G. Serra, D. De Rossi, *Smart Mater. Struct.* **2005**, *14*, 1210.
[255] F. Carpi, A. Migliore, D. De Rossi, *Proc. SPIE* **2005**, *5759*, 64.
[256] F. Carpi, D. De Rossi, *Proc. SPIE* **2006**, *6168*, 61680D.
[257] F. Carpi, D. De Rossi, *Proc. SPIE* **2007**, *6524*, 65240D.
[258] F. Carpi, C. Salaris, D. De Rossi, *Smart Mater. Struct.* **2007**, *16*, S300.
[259] H. F. Schlaak, M. Jungmann, M. Matysek, P. Lotz, *Proc. SPIE* **2005**, *5759*, 121.
[260] M. Matysek, P. Lotz, K. Flittner, H. F. Schlaak, *Proc. SPIE* **2008**, *6927*, 692722.
[261] S. Arora, T. Ghosh, J. Muth, *Sens. Actuators A* **2007**, *136*, 321.
[262] C. G. Cameron, J. P. Szabo, S. Johnstone, J. Massey, J. Leidner, *Sens. Actuators A* **2008**, *147*, 286.
[263] G. Kovacs, L. Düring, *Proc. SPIE* **2009**, *7287*, 72870A.
[264] G. Kovacs, S. M. Ha, S. Michel, R. Pelrine, Q. Pei, *Proc. SPIE* **2008**, *6927*, 69270X.
[265] D. Hanson, V. White, *Proc. SPIE* **2004**, *5385*, 29.
[266] G. Kovacs, P. Lochmatter, M. Wissler, *Smart Mater. Struct.* **2007**, *16*, S306.
[267] F. Carpi, D. De Rossi, *Proc. SPIE* **2005**, *5759*, 16.
[268] F. Carpi, G. Fantoni, P. Guerrini, D. De Rossi, *Proc. SPIE* **2006**, *6168*, 61681A.
[269] E. Biddis, T. Chau, *Med. Eng. Phys.* **2008**, *30*, 403.
[270] S. Dubowsky, S. Kesner, J.-S. Plante, P. Boston, *Ind. Robot: Int. J.* **2008**, *35*, 238.
[271] R. Pelrine, P. S.-Larsen, R. Kornbluh, R. Heydt, G. Koffod, Q. Pei, P. Gravesen, *Proc. SPIE* **2001**, *4329*, 335.
[272] H. Choi, S. Ryew, K. Jung, J. Jeon, H. Kim, J. Nam, A. Takanishi, R. Maeda, K. Kaneko, K. Tanie, *Proc. SPIE* **2002**, *4695*, 138.
[273] K. Jung, H. Nam, Y. Lee, H. Choi, *Proc. SPIE* **2004**, *5385*, 357.
[274] R. Pelrine, R. Kornbluh, Q. Pei, S. Stanford, S. Oh, J. Eckerle, *Proc. SPIE* **2002**, *4695*, 126.
[275] "*Experimental Robotics: The 11th International Symposium, Springer Tracts in Advanced Robotic*, O. Khatib, V. Kumar, G. J. Pappas, Eds., Vol. 54, Springer Science+Business Media B.V., Berlin, Germany 2009, p. 25.
[276] R. Heydt, R. Kornbluh, J. Eckerle, R. Pelrine, *Proc. SPIE* **2006**, *6168*, 61681M.
[277] S. Chiba, M. Waki, R. Kornbluh, R. Pelrine, *Proc. SPIE* **2007**, *6524*, 652424.
[278] M. Aschwanden, A. Stemmer, *Proc. SPIE* **2007**, *6524*, 65241N.
[279] M. Aschwanden, D. Niederer, A. Stemmer, *Proc. SPIE* **2008**, *6927*, 69271R.
[280] H. Kim, J. Park, N. H. Chuc, H. R. Choi, J. D. Nam, Y. Lee, H. S. Jung, J. C. Koo, *Proc. SPIE* **2007**, *6524*, 65241V.
[281] S. Lee, K. Jung, J. Koo, S. Lee, H. Choi, J. Heon, J. Nam, H. Choi, *Proc. SPIE* **2004**, *5385*, 368.
[282] K. Ren, S. Liu, M. Lin, Y. Wang, Q. M. Zhang, *Proc. SPIE* **2007**, *6524*, 65241G.
[283] I. M. Koo, K. Jung, J. C. Koo, J.-D. Nam, Y. K. Lee, H. R. Choi, *IEEE Trans. Robotics* **2008**, *24*, 549.
[284] F. Carpi, A. Mannini, D. De Rossi, *Proc. SPIE* **2007**, *6927*, 692705.
[285] F. Carpi, A. Khanicheh, C. Mavroidis, D. De Rossi, *"2008 IEEE/RSJ International Conference on Intelligent Robots and Systems"* Nice, France, September 22–26, 2008, p. 137.
[286] F. Carpi, A. Khanicheh, C. Mavroidis, D. De Rossi, *IEEE/ASME Trans. Mech.* **2008**, *13*, 370.
[287] K. Tadakuma, L. M. DeVita, J. S. Plante, Y. Shaoze, S. Dubowsky, *"2008 IEEE International Conference on Robotic and Automation"* Pasadena, CA, USA, May 19–23, 2008, p. 2503.
[288] F. Xia, S. Tadigadapa, Q. M. Zhang, *Sens. Actuators* **2006**, *125*, 346.
[289] Y.-Y. Jhong, C.-M. Huang, C.-C. Hsieh, C.-C. Fu, *Proc. SPIE* **2007**, *6524*, 65241Y.
[290] C. Bolzmacher, J. Biggs, M. Srinivasan, *Proc. SPIE* **2006**, *6168*, 616804.
[291] S. Michel, C. Dürager, M. Zobel, E. Fink, *Proc. SPIE* **2007**, *6524*, 65241Q.
[292] S. Michel, A. Bormann, C. Jordi, E. Fink, *Proc. SPIE* **2008**, *6927*, 69270S.
[293] W.-P. Yang, L.-W. Chen, *Smart Mater. Struct.* **2008**, *17*, 015011.
[294] W.-P. Yang, L.-Y. Wu, L.-W. Chen, *J. Phys. D: Appl. Phys.* **2008**, *41*, 135408.
[295] L.-Y. Wu, M.-L. Wu, L.-W. Chen, *Smart Mater. Struct.* **2009**, *18*, 015011.
[296] M. Beck, R. Fiolka, A. Stemmer, *Opt. Lett.* **2009**, *34*, 803.
[297] M. Beck, M. Aschwanden, A. Stemmer, *J. Microsc.* **2008**, *232*, 99.
[298] R. Pelrine, R. Kornbluh, J. Eckerle, P. Jeuck, S. Oh, Q. Pei, S. Stanford, *Proc. SPIE* **2001**, *4329*, 148.
[299] US 6,768,246 B2 (2004), SRI International. R. E. Pelrine, R. D. Kornbluh, J. S. Eckerle, S. E. Stanford, S. Oh, P. E. Garcia.
[300] [300a]WO WO 2007/130252 A2 (2007) SRI International R. D. Kornbluh, R. E. Pelrine, H. Prahlad, S. Chiba, J. Eckerle, B. Chavez, S. E. Stanford, T. Low; [300b] WO 2007/130253 A2 (2007) SRI International R. D. Kornbluh, R. E. Pelrine, H. Prahlad, S. Chiba, J. Eckerle, B. Chavez, S. E. Stanford, T. Low.
[301] S. Chiba, M. Waki, R. Kornbluh, R. Pelrine, *Proc. SPIE* **2008**, *6927*, 692715.
[302] C. Jean-Mistral, S. Basrour, J.-J. Chaillout, *Proc. SPIE* **2008**, *6927*, 692716.
[303] M. Waki, S. Chiba, R. Kornbluh, R. Pelrine, U. Kunihiko, *OCEANS 2008—MTS/IEEE Kobe Techno-Ocean* April 8–11, 2008, p. 1.
[304] S. J. A. Koh, X. Zhao, Z. Suo, *Appl. Phys. Lett.* **2009**, *94*, 262902.
[305] C. Jean-Mistral, S. Basrour, J. J. Chaillout, A. Bonvilain, *DTIP 2007* Stresa, Italy, April 25–27 2007.
[306] C. M. Ihlefeld, Zhihua Qu, *Proc. SPIE* **2008**, *6927*, 69270R.
[307] M. Rosenthal, N. Bonwit, C. Duncheon, J. Heim, *Proc. SPIE* **2007**, *6524*, 65241F.
[308] B. O'Brien, J. Thode, I. Anderson, *Proc. SPIE* **2007**, *6524*, 652415.
[309] C. Keplinger, M. Kaltenbrunner, N. Arnold, S. Bauer, *Appl. Phys. Lett.* **2008**, *92*, 192903.
[310] K. Jung, K. J. Kim, H. R. Choi, *Sens. Actuators A* **2008**, *143*, 343.
[311] K. Jung, K. J. Kim, H. R. Choi, *Proc. SPIE* **2008**, *6927*, 69271S.
[312] N. H. Chuc, D. V. Thuy, J. Park, D. Kim, J. Koo, Y. Lee, J.-D. Nam, H. R. Choi, *Proc. SPIE* **2008**, *6927*, 69270V.

Macromolecular Journals
DOI: 10.1002/marc.200900425